Vol. 584: 119–143, 2017
https://doi.org/10.3354/meps12325

MARINE ECOLOGY PROGRESS SERIES
Mar Ecol Prog Ser

Published December 7

Understanding the life cycle of North Sea brown shrimp *Crangon crangon*: a simulation model approach

Axel Temming*, Claudia Günther, Chris Rückert, Marc Hufnagl

Institute of Hydrobiology and Fishery Science, University of Hamburg, Olbersweg 24, 22767 Hamburg, Germany

ABSTRACT: A simulation model of the life cycle of *Crangon crangon* tracking daily cohorts from the egg stage to the adult stage was programmed in R taking into account size-specific, seasonally varying natural mortality rates of all life stages, temperature-dependent development rates of eggs and larvae, juvenile and adult growth rates as a function of temperature and size, sex, maturation, egg production, and seasonally varying size-specific fishing mortalities. The observed seasonal patterns of commercial catch and egg production could only be reproduced with fast growth rates, which linked winter egg production with the subsequent juvenile recruitment in May–June, the commercial catch peak in September and the peak in egg production over the following winter. Likewise, substantially lowered natural mortalities in winter are essential to generate seasonal patterns similar to the observed ones. The seasonal pattern of egg production can only be reproduced with a minimum spawning age. Cohorts from summer eggs rapidly follow the earlier winter egg cohorts, forming an annual joint wave of growing shrimp. The summer egg cohort originates from summer eggs of the previous year and, depending on winter and spring mortality levels, also from large individuals of the preceding winter egg cohort. The model represents a new tool to investigate maximum yield per recruit in this species as a function of seasonal effort levels, mesh sizes and seasonal closures under different predation and temperature scenarios.

KEY WORDS: Brown shrimp · North Sea · Life cycle · Simulation model · Growth · Mortality · Maturity · Sex · Cohort structure

INTRODUCTION

While population modelling with a focus on stock assessment is widely applied for fish species, comparatively less effort is spent on invertebrate species. Cadrin et al. (2004) stated that for pandalid species, shrimp biologists tend to focus on the variability and complexity of their life histories, whereas population modellers tend to simplify the same processes and ignore abiotic influences. Cadrin et al. (2004) advocate an interdisciplinary approach to shrimp stock assessment in which complex biological information is incorporated into models and sensitivity analyses are conducted to identify critical model components to refine biological and fishery research programs.

Tropical fish and crustacean species face the same problem, in that standard age-based models cannot account for their key features, such as short life span, seasonality of growth, multiple recruitment waves and a sigmoid selection pattern that spans most of the size range of these species. Here, we present a modelling framework that can be viewed as a further step into the 'tropicalisation' of Beverton & Holt—a term introduced by Pauly (1998) to describe the need for the integration of seasonality of growth and sigmoid selection curves into the original concepts of Beverton & Holt (1957). These are preconditions to the successful application of yield-per-recruit concepts for tropical fish and invertebrate species. Our case study, however, focuses on a boreal inverte-

*Corresponding author: atemming@uni-hamburg.de

brate, which shares the same life cycle complications listed above.

Brown shrimp *Crangon crangon* is a dominant epibenthic species in the southern North Sea that plays a central role in coastal food webs. While juvenile *C. crangon* are preyed on by a wide variety of small predatory fish (Tiews 1978), adult *C. crangon* are eaten in huge quantities mainly by juvenile cod *Gadus morhua* and whiting *Merlangius merlangus* (Welleman & Daan 2001, Temming & Hufnagl 2015). *C. crangon* itself preys on a variety of benthic invertebrates (Plagmann 1939, Oh et al. 2001, Feller 2006), but is also reported to control the recruitment of both bivalves (Beukema & Dekker 2014) and flatfish (van der Veer et al. 1991).

C. crangon productivity is sufficiently large enough to support one of the largest North Sea fisheries with about 600 vessels. In 2005, landings exceeded 37 000 tonnes (ICES 2006). North Sea-wide commercial catches have increased from about 20 000 t in the 80s and 90s to well above 30 000 t in recent decades. There are strong indications that reduced predation pressure and increasing fishing effort have contributed to this increase in catches (Temming & Hufnagl 2015), while the possible roles of improved recruitment and better growth conditions remain unclear. Despite the high number of vessels and the use of bottom gear with very small mesh sizes and high discard rates, the fishery is nevertheless unmanaged, having neither quotas nor effort restrictions. No advice is requested from the International Council for the Exploration of the Sea (ICES) by national governments, and consequently national fisheries research institutes allocate little if any scientific resources to the investigation of this species and its fishery.

Large knowledge gaps still exist, even with regard to basic features of the life cycle. An example that has caused controversy over several decades is the quantitative contribution of the different seasonal egg production periods to the main catches in autumn and to the production of new recruits. The different suggestions for the dominant reproduction period generating recruits to the fishing peak in autumn in a given year (X) range from summer egg production of the same year (X) (Boddeke & Becker 1979) to winter egg production (November X – 1 until March X) (Kuipers & Dapper 1984) and more recently to the summer egg production of the preceding year (X – 1) (Campos et al. 2009). The wide range of possibilities is mainly due to uncertainties in growth rates, but also reflects the lack of analysis of the interaction of growth and mortality. Mortality was not considered in the models of Kuipers & Dapper (1984) or Campos et al. (2009).

The unresolved debate served as a starting point for the development of a model aimed at a quantitative integration of the different biological processes into a life cycle model. This effort led to a first model version (Temming & Damm 2002), which was designed to relate the seasonal egg production to the seasonal pattern of recruitment of 15 mm juveniles on the tidal flats using temperature-dependent egg and larval development rates and juvenile growth rates. The main conclusions were that (1) the first strong recruitment wave in the German Wadden Sea originates from the preceding winter egg production and (2) German water temperatures were too low to explain the occurrence of the peak in May–June.

From this starting point, 2 different directions were followed: (1) the integration of the simple model into 3D ocean models to better understand the timing of recruitment resulting from the interaction of locally different seasonal temperatures and drift (Daewel et al. 2011, Hufnagl et al. 2014) and (2) the extension of the simulation model to include sex-specific adult growth, maturity, egg production, and fishing and natural mortalities by size class and month. We herein only present recent model developments following from the second approach.

First results of the application of an extended female-only model were presented at the Crangon Working Group meeting in 2002 (ICES 2003). A second more complex version was developed by Rückert (2011), while in parallel a series of new growth experiments with sex separation and meta-analyses of published data led to a new growth sub-model (Hufnagl & Temming 2011a,b) and — in combination with field data on length composition — also to improved total mortality estimates (Hufnagl et al. 2010b, 2013). Here, we present the results of this most advanced model version with a focus on the life cycle of brown shrimp.

Over the long period of model development, which started at the end of the 1990s, not only has the model changed, but also some of the central input data, such as temperatures, seasonal patterns of effort and landings, and, most importantly, the ratio between natural (predation) and fishing mortality (Temming & Hufnagl 2015). These changes have, due to the differing seasonal patterns of predation and fishing mortalities, quite far-reaching implications for the population dynamics of brown shrimp. Therefore, the second aim of this study was to disentangle the effects of changing environmental conditions on the seasonal dynamics of the brown

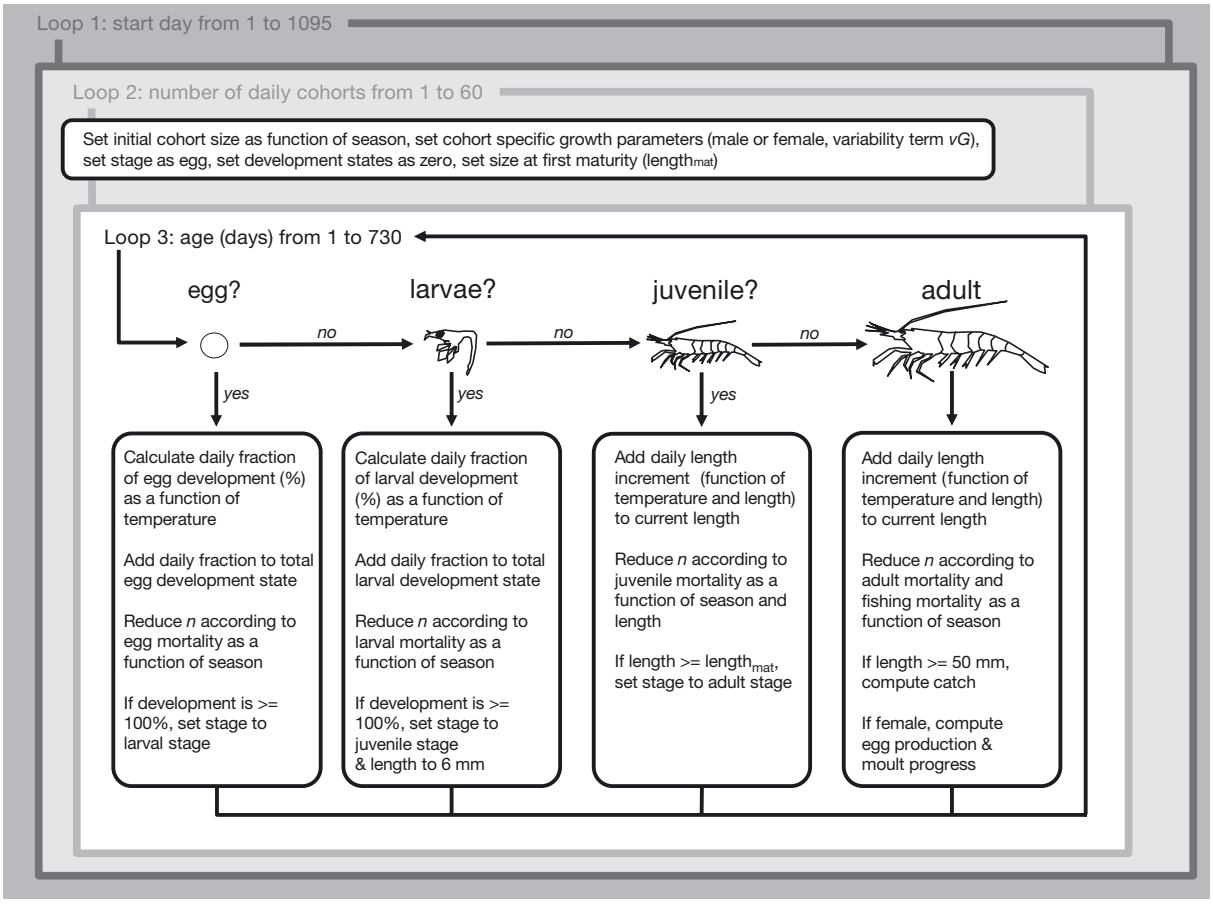

Fig. 1. Basic program structure of the simulation model. *n* = actual number of individuals surviving

shrimp stock using the most advanced model with revised input parameters.

MATERIALS AND METHODS

General model structure and settings

The model was programmed in R and simulates cohorts from the egg stage to the adult stage. The model structure can best be understood as 3 hierarchical loops (Fig. 1, Fig. S1 in the Supplement at www.int-res.com/articles/suppl/m584p119_supp.pdf): the outer loop cycles through 1095 sequential start days. The next nested loop cycles through 60 cohorts, which differ in their respective parameter values to account for sex differences and variability. The innermost loop follows each of the daily cohorts throughout 730 d passing the stages egg, larvae, juvenile and adult. All calculations are conducted in discrete daily time steps using either integrated functions (mortality) with a time interval of 1 d (1/365 yr) or numerical equations (growth) with a t of 1 d. All cohorts are computed sequentially and the results are subsequently aggregated for the whole population in different result categories (e.g. catches, biomass, recruits and egg production). Results are presented for the last year, when equilibrium conditions are approached and all size and age classes are present.

Egg and larvae

The initial size of each daily cohort, which is equivalent to the number of fertilized eggs, is set as proportional to a seasonal spawning index inferred from the daily egg production intensity (see 'Initial size of daily cohorts'). Each day, a temperature (T, in °C)-dependent fraction of the total development of either the egg or the larvae (= 100 %) is added to the previously reached state (= percentage) of development. Egg and larval numbers are reduced each day with the respective natural mortality rate (see 'Mortality').

Table 1. Parameters and settings of standard run (SR) I and SR II. *sM*: relative seasonal mortality depending on life-stage; juv1: juvenile shrimp with length range 5–20 mm; juv2: juvenile shrimp with length range 20–50 mm; BSH: Bundesamt für Seeschifffahrt und Hydrographie (German Federal Maritime and Hydrographic Agency)

Line #	Parameter/setting	Unit	SR I	Source	SR II	Source
1	Spawning index (monthly mean)		1.01; 1.07; 0.37; 0.91; 1.46; 1.92; 2.28; 1.01; 0.41; 0.32; 0.52; 0.73	This study	0.62; 0.38; 0.41; 0.98; 1.61; 2.20; 2.51; 1.37; 0.41; 0.29; 0.62; 0.61	This study
2	Start number	n	24×10^9	This study	3.5×10^9	This study
3	Adult mortality (M)	yr^{-1}	3.3	Temming & Hufnagl (2015)	1.5	Temming & Hufnagl (2015)
4	Seasonal mortality (sM) index sM_{larvae} (monthly mean)		0.23; 0.23; 0.27; 0.28; 0.56; 1.13; 1.69; 2.26; 2.26; 1.69; 1.13; 0.28	Rückert (2011)	See SR I	Rückert (2011)
5	sM_{juv1} (5–20mm)		0.22; 0.22; 0.27; 0.28; 0.57; 1.13; 1.69; 2.26; 2.26; 1.69; 1.12; 0.28	Rückert (2011)	See SR I	Rückert (2011)
6	sM_{juv2} (20–50mm)		0.25; 0.25; 0.29; 0.29; 0.50; 1.08; 1.64; 2.20; 2.24; 1.78; 1.16; 0.33	Rückert (2011)	See SR I	Rückert (2011)
7	sM_{adult} (>50mm)		0.33; 0.33; 0.33; 0.33; 0.33; 0.96; 1.50; 2.02; 2.14; 2.02; 1.26; 0.45	Rückert (2011)	See SR I	Rückert (2011)
8	Fishing mortality (F)	yr^{-1}	2.2	Temming & Hufnagl (2015)	3.8	Temming & Hufnagl (2015)
9	Seasonal fishing effort index (sF) (monthly mean)		0.04; 0.04; 0.31; 1.41; 1.41; 1.41; 1.41; 1.41; 1.41; 1.41; 1.41; 0.31;	Rückert (2011)	0.19; 0.20; 0.86; 1.60; 1.39; 1.26; 1.19; 1.25; 1.27; 1.26; 1.09; 0.45	ICES (2014)
10	Temperature larval stage (T_{larvae}) (monthly mean)	°C	4.54; 3.09; 3.15; 5.14; 8.66; 12.80; 15.72; 17.00; 16.22; 14.06; 10.54; 7.12	Fonds (1978), Rückert (2011)	6.03; 5.31 ;5.40; 7.11; 10.21; 13.73; 16.83; 18.02; 17.29; 15.12; 11.75; 8.53	BSH (2002–2012)
11	Temperature other life-stages (T_{others}) (monthly mean)	°C	5.53; 5.12; 4.71; 8.22; 12.53; 16.23; 17.64; 17.75; 16.29; 14.49; 10.73; 7.67	Rückert (2011)	5.43; 4.34; 4.85; 8.80; 13.56; 16.53; 18.78; 19.04; 17.09; 14.85; 11.23; 8.01	BSH (2002–2012)

Juveniles

Juveniles and adults grow depending on temperature (in °C) and body length (total length in mm). In juveniles and adults, a daily size increment is added to the current length (see 'Development and growth'). The present version simulates the female and male part of the population separately.

Cohorts with shrimp smaller 50 mm are diminished by a seasonal length-dependent mortality (see 'Mortality'). Natural mortality is highest during the earliest and smallest life stages and decreases as shrimps become larger.

Adults

If shrimp exceed a length of 50 mm, fishing mortality is added to natural mortality. Both fishing and natural mortality follow a seasonal pattern. Each female cohort has a randomly chosen length at first maturity assigned and after reaching this size, egg production is simulated as well (see 'Egg production').

Initial size of daily cohorts

The number of eggs starting in the simulation was calculated as the product of (1) a relative spawning index (Table 1, line 1), which reflects the seasonal variation of egg production and (2) a start number (Table 1, line 2) representing the mean number of individuals starting each day as an egg. The start number is tuned to adjust the yield-per-recruit model to a specific amount of landings per year.

The relative spawning index is calculated on a monthly basis derived from the spawning intensity

(*SI*) following the seasonal egg production proxy given by Temming & Damm (2002):

$$SI = C \times \sum_{L=50}^{L_{max}} (N_L \times E_L \times EF_L \times MF_{L,T}) \quad (1)$$

C is an estimate of the relative seasonal stock size, *N* is the fraction of each size class (*L*) in *C*, *E* is the share of egg bearing females per size class, *EF* is the mean number of eggs per size class and *MF* is the moulting frequency in moults per day as a function of size class (*L*) and temperature (*T*). Stock size (*C*) was approximated using commercial landings per unit effort, and the size structure (*N*) of shrimp >50 mm and the share of egg bearing females (*E*) were extracted from by-catch samples (Tiews 1990). Egg numbers per female (*EF*) size class were derived from a function of Havinga (1930):

$$EF = 0.01878 \times L^{3.539} \quad (2)$$

A recent study on egg sizes of *Crangon crangon* demonstrated seasonal changes in egg sizes and also differences between 2 years (1996 and 2009); however, no update on the shrimp size–egg number relation is given nor are deviations from Havinga's data reported (Urzua et al. 2012). The share of moulting females (*MF*) was calculated as the reciprocal value of the temperature- and length-dependent intermoulting period (*IM*) given by Hufnagl & Temming (2011b):

$$IM = 5.7066 \times L^{0.7364} \times T^{-0.09363} \quad (3)$$

The resulting monthly values of the spawning intensity were standardized to the mean and interpolated to a daily spawning index.

Development and growth

Temperature-dependent egg development time (D_{egg}) in days was calculated as in Redant (1978) based on data from Wear (1974) and Havinga (1930):

$$D_{egg} = 1031.34 \times T^{-1.354} \quad (4)$$

Using the reciprocal of this equation, the fractional contribution of egg development per day was calculated based on the respective temperature. This allows variable egg development under changing temperature conditions. If the sum of the fractions exceeds the value 1, the egg development is completed and the cohort enters the larval stage. The time for larval development (D_{larvae}) is likewise described as a function of temperature following Criales & Anger (1986):

$$D_{larvae} = \left[\left(\frac{5.5}{0.00584}\right) \times T^{-1.347}\right] \quad (5)$$

The calculations for larval development follow the same scheme that was applied for the egg development. When the larval stage is completed, shrimp start into the juvenile stage with a fixed length of 6 mm.

For the growth of juvenile and adult shrimp, we tested 2 growth models. In the first equation, growth was modelled in the same way as described in Temming & Damm (2002) for juvenile shrimps implementing the growth parameters of Kuipers & Dapper (1984) (see Table 2). The daily length increment was calculated from the first derivative of the von Bertalanffy growth equation:

$$\frac{\Delta L}{\Delta t} = E - K \times L \quad (6)$$

with

$$E = a + b \times T \quad (7)$$

Here, *a*, *b* and *K* are coefficients from experiments measuring length increments in mm per day. In the second approach, Eq. (6) was extended to give a physiologically more realistic representation of the catabolic term *K*, which is typically exponentially temperature dependent:

$$\frac{\Delta L}{\Delta t} = a + b \times T - c \times e^{d \times T} \times L \quad (8)$$

Here, *a*, *b*, *c* and *d* are coefficients. ΔL is calculated per day with $\Delta t = 1$ d. Parameter settings were based on Hufnagl & Temming (2011b), who performed a comprehensive literature study on growth of brown shrimp. Female and male growth (Table 2) was modelled separately in both standard runs (see 'Standard run I' and 'Standard run II').

Growth variability and selective survival

Growth variability is high in *C. crangon* and since mortality most likely decreases with size, this may lead to increased survival of faster-growing individuals (Hufnagl & Temming 2011b). To implement selective survival in the simulation model, multiple daily cohorts start with slightly different growth rates. Growth variability was included by multiplying the complete growth equation by a random number. This random number (*vG*) is cohort specific and drawn from a normal distribution with mean 1 and standard deviation 0.3. The distribution was truncated at 3 times the standard deviation to avoid unrealistic strong growth. Thereby, we used a fixed set of random numbers to ensure comparability of different runs, which follows a smooth Gauss curve.

Table 2. Settings and descriptions of scenario runs. All scenarios base on standard run (SR) I. In the group D scenarios, settings were sequentially changed from SR I to SR II. G_{mean}: mean growth; G_{max}: maximal growth rate

Scenario	General	Figure	Details					
			Equation	*a*	*b*	*K* (Eq. 6), *c* (Eq. 8)	*d*	Source
A.1	Growth	2, 3	6	0.1625	0.01025	0.00403	–	Kuipers & Dapper (1984)
A.2	Growth	2, 3	8	0	0.02421	0.00115	0.08492	Hufnagl & Temming (2011b) (G_{mean})
A.3	Growth	2, 3	8	0	0.03054	0.00104	0.09984	Hufnagl & Temming (2011b) (G_{max})
SR I / SR II	Growth female	2, 3	8	0	0.04028	0.00193	0.0877	Hufnagl & Temming (2011b)
SR I / SR II	Growth male	2, 3	8	0	0.03424	0.002	0.0877	Hufnagl & Temming (2011b)
B.1	Mortality	5	Seasonal constant natural mortality (*M*)					
B.2	Mortality	4, 5	*M* and *F* estimated for the 2000s					Temming & Hufnagl (2015)
C.1	Temperature	5	Temperature datasets for the 2000s					See text
C.2	Spawning	5	Without minimum spawning age					See text
			Change #1	Change #2	Change #3	Change #4		
D.1	SRI to SR II	6	Spawning index					
D.2	SRI to SR II	6	Spawning index	Seasonal *F*				
D.3	SRI to SR II	6	Spawning index	Seasonal *F*	Temperature			See text
D.4	SRI to SR II	6	Spawning index	Seasonal *F*	Temperature	*M*/*F* ratio		

Mortality

Natural exponential mortality rate *M* was included in a 2-step approach. First, a length- and stage-dependent mortality level was estimated. In a second step, length- and stage-dependent mortalities were multiplied with a monthly based index reflecting the seasonal variation of natural and fishing mortality (see 'Seasonality of mortality').

Since eggs are attached to females, they have the same mortality as adult female shrimps (Table 1, line 3).

Larval mortality is estimated from the allometric equation of Peterson & Wroblewski (1984):

$$M_{larvae} = 1.22 \times 1.5758 \times DW_{ZS}^{-0.25} \quad (9)$$

Dry weights (*DW*) of the larval zoea stages (DW_{ZS}) were taken from Criales & Anger (1986):

$$DW_{ZS} = e^{2.7 + 0.222 \times ZS} \times 10^{6} \quad (10)$$

M for sizes between 6 mm and the beginning of the adult stage (with 50 mm) was interpolated between the *M*-level in the latest larval stage (M_6) and *M* for adult shrimp (*M*) assuming a nonlinear decrease with length:

$$M_{juv} = e^{\ln(M_6) + [\ln(L) - \ln(6)] \times \frac{\ln(M) - \ln(M_6)}{\ln(50) - \ln(6)}} \quad (11)$$

As a consequence of this interpolation, the adult *M*-level influences the *M* of juveniles. The total *M*-levels for adult shrimp were estimated independently from the updated growth data and size compositions of scientific surveys and by-catch sampling programs using length-based methods (Hufnagl et al. 2010b, 2013). Total mortality levels of the respective decades were split into the fishing mortality rate (*F*) and *M* based on the relation of total predation and total catch (Temming & Hufnagl 2015; see 'Standard run I' and 'Standard run II').

The respective season- and size-specific total mortalities (*M*) were used to reduce the cohort size in the daily time steps:

$$N_{i+1} = N_i \times e^{-(F+M) \times \left(\frac{(1)}{365}\right)} \quad (12)$$

with N_i indicating the cohorts size at the start of the day *i*.

Seasonality of mortality

With a constant *M* in all months (see 'Results'), it was impossible to reproduce the observed seasonal

catch and population patterns. It was therefore essential to construct a mortality matrix with seasonally varying *M*-levels (Table 1, lines 4–7). These seasonal patterns were based on the assumptions that (1) seasonal changes in natural mortality follow a continuous and unimodal pattern, (2) seasonal changes for the smallest stages roughly follow the temperature pattern of the season, and (3) seasonal changes in natural mortality of juvenile and adult shrimp should reflect information on seasonal predation by the 2 most important predators, whiting and cod. For the different size groups, the following settings were made. The mortalities for larvae were approximately scaled in proportion to temperature based on the general assumption that the turnover in the pelagic system is correlated with temperature and the observation that biomasses of potential predators, namely jellies and juvenile sprat and herring, are highest in summer in the coastal waters of the SE North Sea (Greve & Reiners 1988, Dänhardt 2010, Jansen 2002). The same seasonal mortality pattern as that for larvae was applied to the first juvenile stage, including shrimps of 6 to 20 mm length. Maximum mortalities for the second juvenile stage (20–50 mm) were slightly shifted into late summer and autumn compared with the index of larvae and early juveniles, as maximum consumption of shrimps (with length from 15 to 50 mm) by whiting and cod in the northern German Wadden Sea is found between August and October (Jansen 2002). From stomachs sampled in coastal areas outside of the Wadden Sea in combination with consumption estimates using the multispecies virtual population dynamics model for the North Sea, the consumption of adult brown shrimp (>50 mm) was estimated for all 4 quarters of a year for cod and whiting (Temming & Hufnagl 2015).

For the seasonal variation in fishing mortality, we used a monthly index based on effort data of the German fishery (see Table 2, line 9).

Egg production

The number of eggs produced per time interval by a cohort is a product of 3 terms: the number of mature females in the population, the share of moulting females and the length-dependent number of eggs carried per female (Eq. 2). The number of mature females is calculated with size at first maturity as a cohort-specific value, which is determined when the cohort starts into the model. Between cohorts, sizes at first maturity vary randomly in such a way that the average pattern of field observations of the proportion of egg-bearing females relative to all shrimps in a given length class (Neudecker & Damm 1992) is reproduced. The figures were corrected for the share of males per length class based on data in Martens & Redant (1986). The function was adjusted such that the proportion of egg-bearing females was 100% for the largest shrimps. The resulting logistic equation describing the proportion of mature females (P_{mat}) as a function of length (L) was inverted to the following form:

$$\text{length}_{mat} = 45.7 + \frac{1}{0.244} \times \ln\left(\frac{P_{mat}}{99.5 \times 0.076 - 0.076 \times P_{mat}}\right) \quad (13)$$

Lengths at first maturity (L_{mat}) were calculated for all daily cohorts with a random number between 0 and 100 for P_{mat}.

As spawning was assumed to be synchronized to the moulting events, the moulting process was modelled to trigger fertilisation and egg/larval release. Although growth in length and moulting are coupled processes in reality, intermoult periods in the simulation were calculated independently. The reciprocal of Eq. (3) was used to estimate the fraction of shrimps moulting per day in a cohort.

It turned out to be impossible to reproduce the seasonal egg production pattern that was used as input spawning index without including a minimum age of spawning in the simulation (see 'Results'). This minimum age for spawning shrimp was set to 180 d since the end of the larval stage, which gave the closest correspondence to observed data.

Temperature

The simulation model was run previously with different sets of historical temperature data (Table S1 in the Supplement at www.int-res.com/articles/suppl/m584p119_supp.pdf). During this study, we applied 2 temperature sets. In standard run (SR) I, we applied temperature data used in the final run of Rückert (2011). All life stages are assumed to migrate between coastal and deeper areas in the German Bight, essentially utilizing at any time the warmer temperature of 2 different time series (1960–1995): (1) Helgoland Roads (54° 11′ N, 7° 53′ E), and (2) coastal temperatures (Büsum Harbour, 54° 07′ N, 8° 51′ E). Rückert (2011) assumes that larvae experience offshore temperatures of the Netherlands (data from 1960–1962, 1964), while they drift into the German Bight. Thus, SR I is based on temperature data from the 1960s to the 1990s (see Table 1 for mean monthly values).

In SR II, we focused on water temperatures from the last decade but followed the same assumptions about ambient temperatures of the larvae as in SR I. We employed daily mean values (2002–2012) of the measurement station 'Ems' (54° 10′ N, 6° 21′ E) of the German Federal Maritime and Hydrographic Agency (BSH) in 6 m water depth for the larval life stage. For all other life stages, the warmer temperature of the following 2 time series (2002–2012) was chosen: (1) bottom temperatures in the German Bight (measurement station 'Deutsche Bucht', 54° 10′ N, 7° 27′ E), and (2) and the coastal temperatures (Büsum Harbour, 54° 07′ N, 8° 51′ E, see Table 1 for mean monthly values).

Validation data

Three aggregated model outputs were compared with observational data to judge the performance of the model: (1) the seasonal pattern of monthly landings, (2) the occurrence of 15 mm recruits and (3) seasonal egg production.

We calculated monthly catches of shrimps >50 mm that died from fishing mortality in the model by summing up the number of shrimps per 1 mm length class and multiplying it by the corresponding weight of that length class following the length (mm) – weight (g) relationship published by Hufnagl et al. (2010a):

$$W = 4.625 \times 10^{-6} \times L^{3.084} \quad (14)$$

This simulated seasonality of catches from SR I and SR II was compared with the seasonal monthly patterns of commercial catches of the German fleet (ICES 2013) during the period from 1980 to 1999 and the last decade (2002–2012), respectively. The size of the number of individuals starting into the model as an egg was adjusted to meet the average yearly overall size of commercial catches (Table 1, line 2). In all scenario runs, the start number of SR I was used.

The size composition of the catch resulting from SR I and II are binned in 5 mm length classes and compared with data from 2 different sources: (1) the mean length frequency of a by-catch sampling program (Tiews 1990) including the years from 1980 to 1994 and (2) the mean length frequency of the Demersal Young Fish Survey (Siegel et al. 2008) including the years from 2002 to 2012. This comparison is only performed for September catches due to the availability of survey data.

Field data on the temporal occurrence of small shrimps (ca. 5–25 mm) on the tidal flats of the German Wadden Sea were compiled by Temming & Damm (2002). They calculated an index standardized to a length of 15 mm using data sampled with pushnets in the years 1986, 1992 and 1993. This seasonal index was compared with the seasonal occurrence of 15 mm recruits from the simulation model. For each daily cohort in the model, the month and the corresponding abundance was registered when the length of 15 mm was attained.

Lastly, the monthly aggregated seasonal pattern of egg production was compared with the seasonal input index used to initiate spawning in the model.

Standard run I

We defined 2 SRs where SR I is based on parameter settings of a previous model version (Rückert 2011) and on field data (seasonal effort pattern, temperatures) from the 2 decades before 2000 (Table 1). The values of F = 2.2 yr^{-1} and M = 3.3 yr^{-1}, which are representative for that period, were taken from Temming & Hufnagl (2015). This run represents the biological conditions of the 1980s and 1990s, when predation mortalities were still high and temperatures were lower. In addition, the seasonal pattern of fishing effort differed to some extent from that of the most recent period.

Standard run II

A second run (SR II) was based on field data from a more recent period and newly available parameter estimates, mainly for the mortality levels F = 3.8 yr^{-1} and M = 1.5 yr^{-1} (Temming & Hufnagl 2015) and the recent seasonal temperature patterns. SR II has 5 differences compared with SR I. (1) The spawning index initiating the seasonality of daily cohorts was calculated with recent temperature data (mean of 2002–2012). (2) Seasonal fishing mortality was adjusted to average seasonal effort data from the last decade (2002–2012). (3) We used recent temperature data (mean of 2002–2012) for all temperature-dependent processes. (4) We used the average M:F ratio estimated for 2002–2012 from Temming & Hufnagl (2015). (5) We used a start number that is adjusted to reproduce the observed amount of recent landings.

Scenario runs

After performing a sensitivity analysis following the protocol of Megrey & Hinckley (2001), which indicated that temperature, growth rate and natural mor-

tality settings have the strongest influence on model outputs (results not shown here), we selected the most influential parameters and settings and varied them in the scenario runs in a systematic fashion. All scenario runs used the general settings of SR I, but varied specific aspects to test in isolation (Table 2) the effects of slow growth rates with Eq. (6) (scenario A.1) in contrast to faster growth rates with Eq. (8) (scenarios A.2 and A.3), the effects of non-seasonality of natural mortality (scenario B.1), changes in the *M*:*F* ratio with constant total mortality (scenario B.2), the effects of the recent temperature data (scenario C.1) and the absence of a minimum spawning size (scenario C.2).

Lastly, we performed a stepwise change from SR I to SR II where scenario D.1 equals SR I but with the revised spawning index, D.2 equals D.1 but in addition the seasonal *F* pattern is updated, while in D.3. the recent temperature data are also applied. D.4 is equivalent to SR II with the exception of the number of eggs starting each day into the model.

Tuning of parameter values

The vast majority of parameter values were used as determined in experiments (development and growth rates) or derived from external data analysis (levels of fishing and natural mortality). There are, however, 2 aspects where tuning was applied: (1) the minimum spawning age was adjusted in 5 d steps to generate a match between simulated and observed spawning intensity and (2) the seasonal differences in natural mortalities of the larval and juvenile stages were introduced to avoid the complete mismatch in seasonal patterns. Instead of a strict optimization, we attempted to generate a set of patterns that reflects our best understanding of the seasonality of the predation processes. For larger juveniles and adults, the seasonality is mostly based on quantitative information on predator densities or even estimated quarterly consumption rates.

RESULTS

Standard run I

Due to the extensive restructuring of the model in the past and the transfer of the code across 4 different programming languages (Pascal, Delphi, Matlab and R), one aim was to reproduce the results of the most complex previous model version. Most settings of SR I were hence equal to those of Rückert's (2011) model version representing the 2 decades prior to 1990. In general, the aggregated monthly outputs of SR I and Rückert's (2011) final run have very similar seasonal patterns (not shown) and model outputs explain a high amount of the variability of Rückert's (2011) model output regarding landings ($r^2 = 0.98$), biomass ($r^2 = 0.92$), recruits ($r^2 = 0.74$) and egg production ($r^2 = 0.89$).

Like previous model versions, SR I is able to reproduce the observed seasonal patterns of landings, recruits and egg production (Fig. 2). Here, seasonal landings of the model can reproduce the minimum catches in winter, the spring level and the maximum values in autumn ($r^2 = 0.95$). The temporal occurrence of recruits on the tidal flats with a peak in June can be reproduced ($r^2 = 0.92$) as well as the summer maximum in egg production ($r^2 = 0.89$) followed by minimal values in autumn.

Growth scenarios

Scenario A.1 represents slow growth based on a simple growth equation (Eq. 6) formulated by Kuipers & Dapper (1984). Here, a cohort starting in the middle of January as a fertilized egg resulted in a length of <45 mm at the end of the first year and 65 mm at the end of the second year (Fig. 3). With this growth model, maximum landings were predicted for July and August and decreased thereafter in autumn (Fig. 2). Likewise, the prediction of the seasonal egg production deviated strongly from the reference data with a shift of the peak from summer to autumn. Growth scenario A.2 representing mean growth still deviates from the reference data and the results of SR I, especially in the seasonal landings data, which are overestimated in late spring and underestimated in autumn. Growth scenario A.3 is closest to the reference data and very similar to the results of SR I. Unsurprisingly, the amount of absolute landings increased with increasing growth rate assuming constant recruitment (results not shown). Compared with scenario A.1, landings are twice as high in scenario A.2 and are more than 5 times higher in scenario A.3.

Mortality scenarios

Natural mortality in SR I and SR II was varied seasonally (Table 1 lines 4–7, Fig. 4) with lower rates from January to June (1.1, 1.5 and 3.0 yr^{-1} for adult, 35 mm and 15 mm shrimp, respectively, in SR I) and a maximum in August–September (7.1, 9.6 and

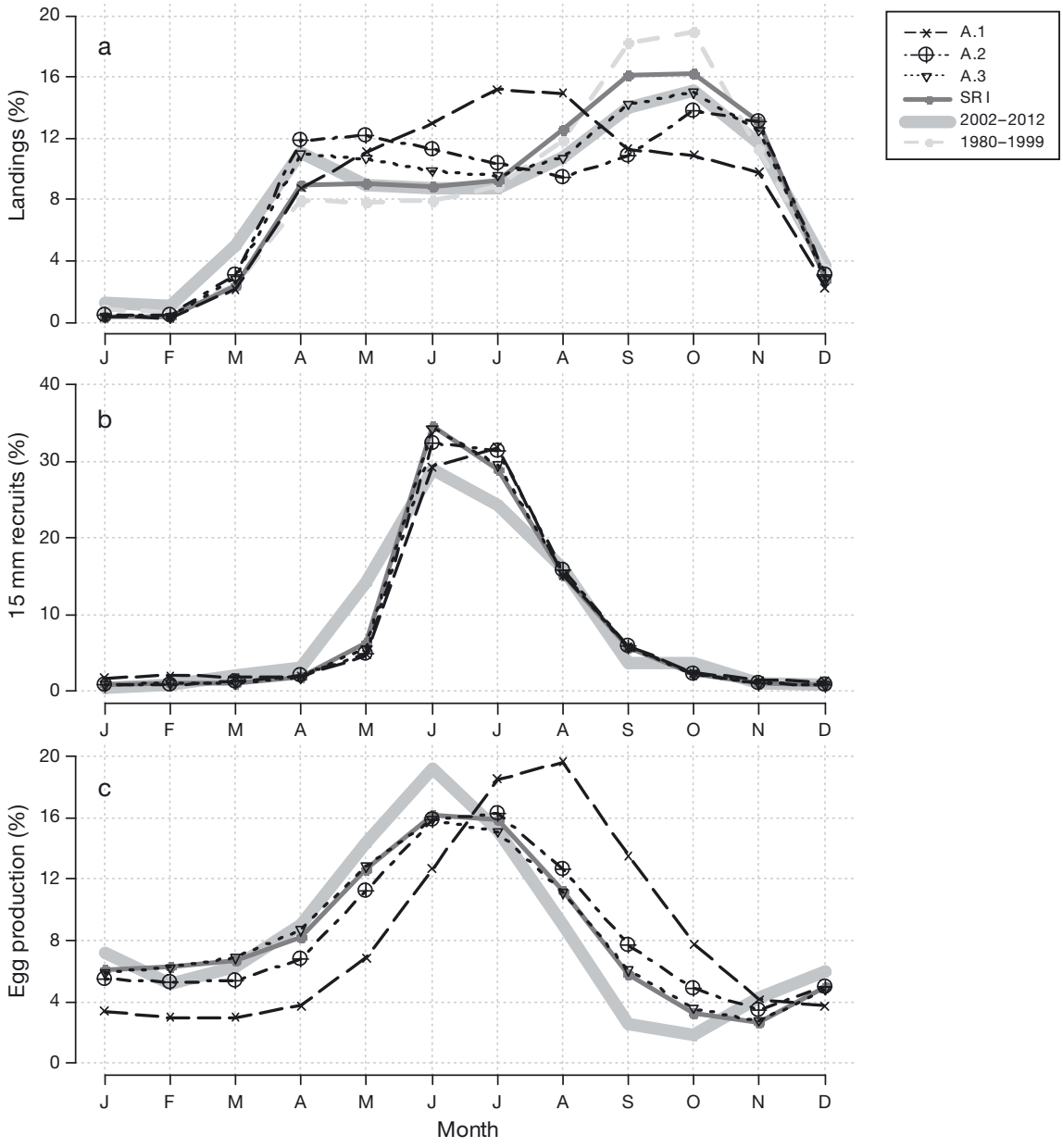

Fig. 2. Seasonal model outputs of different growth scenarios (A.1: slow growth after Kuipers & Dapper 1984; A.2: mean growth after Hufnagl & Temming 2011b; A.3: maximum growth after Hufnagl & Temming 2011b), standard run (SR) I and observational data of (a) landings, (b) 15 mm recruits and (c) egg production. For landings, 2 time series (1980–1999 and 2002–2012) are shown as observational data; catches are displayed for individuals >50 mm

19.7 yr^{-1} for adult, 35 mm and 15 mm shrimp, respectively, in SR I). This seasonality was artificially constructed following the temperature pattern of the season and the abundance of predators (see 'Materials and methods'). Scenario B.1, which assumes a constant M over the year, was not able to reproduce the observed patterns (Fig. 5). Landings during August and September were about 40 and 60% lower than observed, respectively, and the autumn peak was shifted (from October) to November. The peak in recruits was likewise shifted to August. Assuming the same number of individuals that start into the model (e.g. the same recruitment) as in SR I, absolute landings over the year are 3 times higher, indicating the strong influence of the seasonality of natural mortality on total landings.

In scenario B.2, the M:F ratio was shifted from 1.5 (M = 3.3 yr^{-1}, F = 2.2 yr^{-1}) to 0.4 (M = 1.5 yr^{-1}, F = 3.8 yr^{-1}), while keeping total mortality almost constant (Fig. 4). Since the same recruitment numbers were

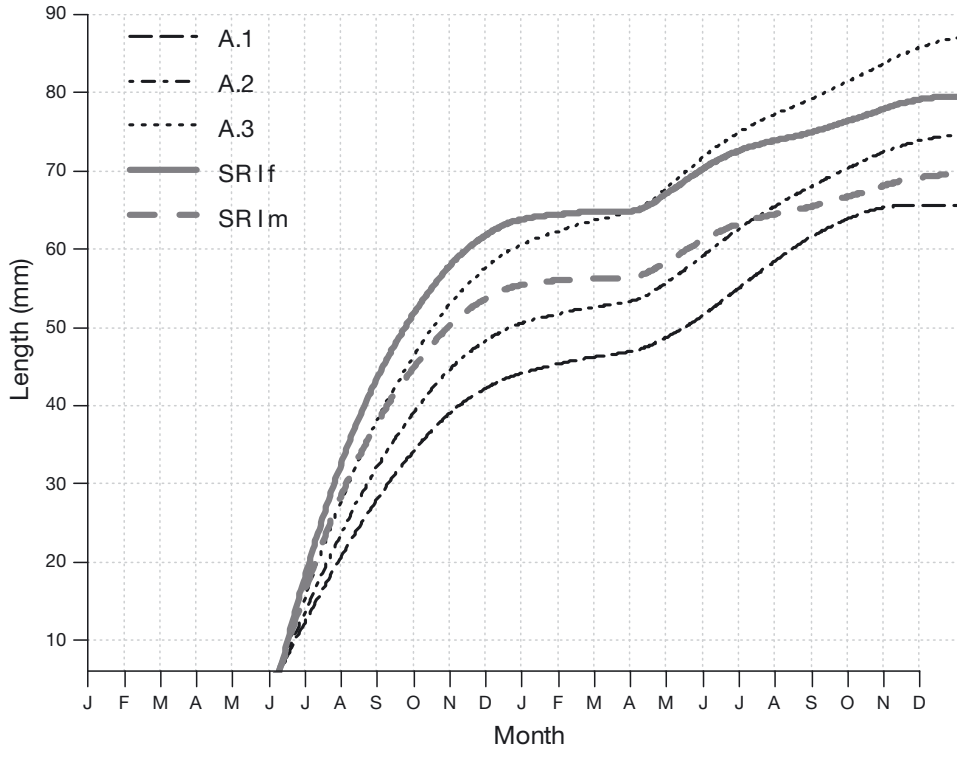

Fig. 3. Growth in length of the mean daily cohort starting its development from a fertilised egg on 15 January (dominant cohort in autumn catches with reference to standard run [SR] II). Growth scenarios A.1 (slow growth after Kuipers & Dapper 1984; Eqs. 1 & 2), A.2 (median growth after Hufnagl & Temming (2011b), Eq. 3) and A.3 (high growth after Hufnagl & Temming 2011b; Eq. 3) and SR I (after Hufnagl & Temming 2011b; f: female; m: male)

used, this setup strongly increased total landings by a factor of 4.3 compared with SR I (not shown) as a consequence of the combined increase in fishing and decrease in natural mortality. However, the effect on the seasonality of aggregated model outputs was limited except for the influence on egg production: seasonality (i.e. a distinct summer peak) in egg production was reduced and eggs are more equally produced over the year. This was a consequence of the increase in total mortality in spring due to the shift from fish to human predators (Fig. 4), increasing the mortality of large females which produce eggs in summer.

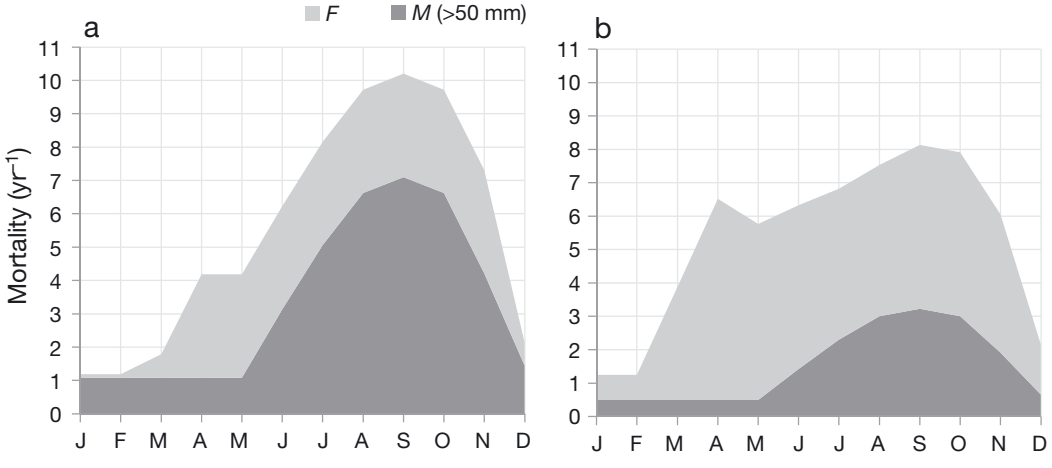

Fig. 4. Seasonal distribution of natural (M) and fishing (F) mortality for shrimps larger 50 mm. (a) Settings of standard run (SR) I with a mean $F = 2.2$ and a mean $M = 3.3$ (average M:F ratio before 2000s). (b) Settings of the mortality scenario B.2 (= SR II) with a mean $F = 3.8$ and a mean $M = 1.5$ (average M:F ratio of the 2000s)

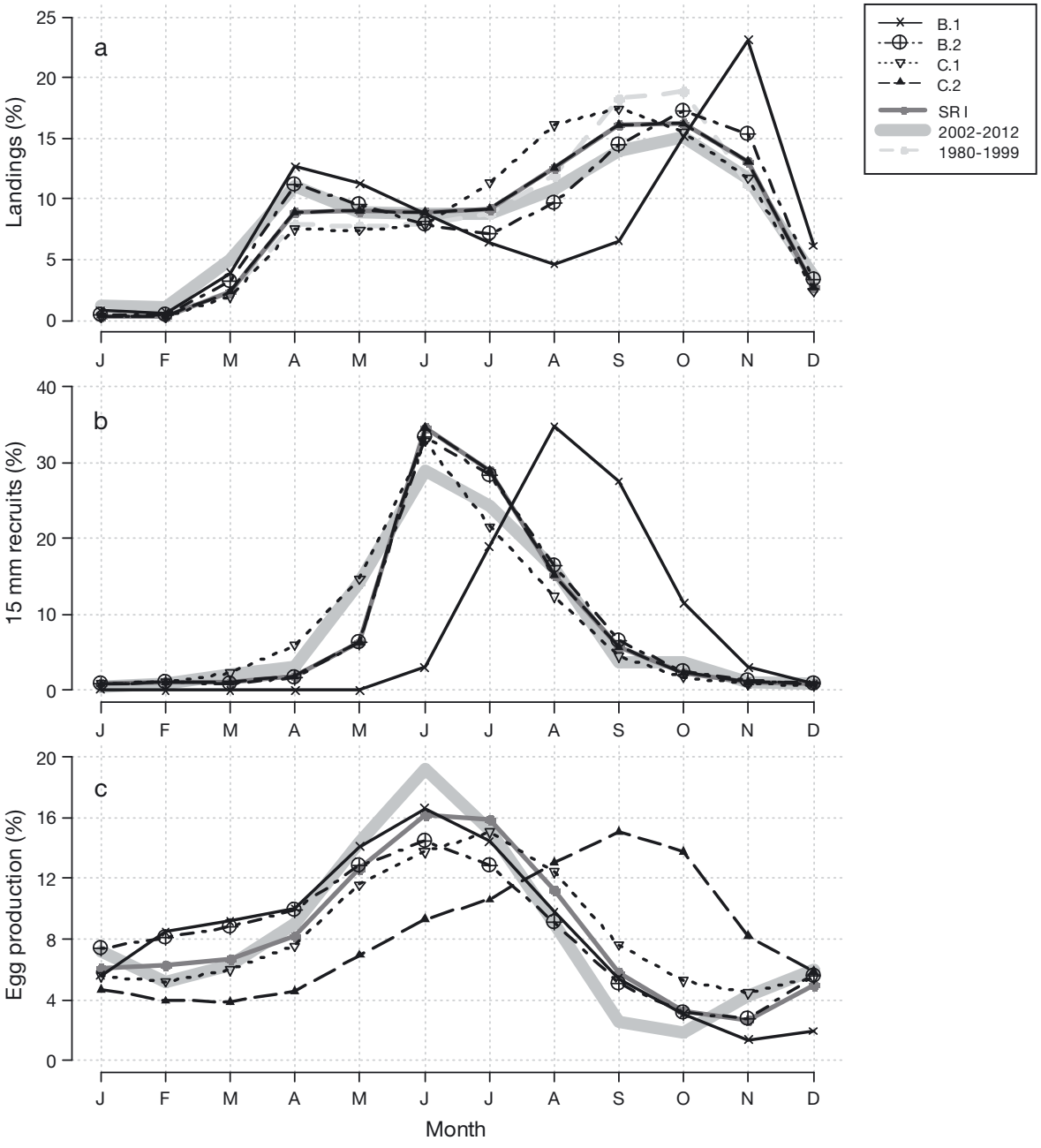

Fig. 5. Seasonal observation data and model outputs of SR I and different scenarios of (a) landings, (b) 15 mm recruits and (c) egg production. B.1: seasonally constant natural mortality; B.2: *M*:*F* ratio changed from 1.5 to 0.4 compared with standard run (SR) I; C.1: temperature dataset of the 2000s; C.2: without minimum spawning age. For landings, 2 time series (1980–1999 and 2002–2012) are shown as observational data; model output catches are displayed for individuals >50 mm

Temperature and minimum spawning age scenarios

In SR I, we applied Rückert's (2011) heterogeneous temperature series, which include data from the 1960s to 1990s for adults and juveniles and data from the 1960s for larvae. Temperature series of the 2000s, which were used in scenario C.1, exhibit overall higher temperatures, especially in winter. Assuming the same recruitment strength as in SR I, total landings increased and doubled in autumn. Like the change in the *M*:*F* ratio (scenario B.2), the increase in temperature leads to a decrease in the seasonality of egg production, increased recruitment in May and a peak landings in August–September instead of September–October (Fig. 5).

In contrast to SR I, which assumes a minimum spawning age of 180 d, the seasonal egg production of scenario C.2 without any minimum spawning age reveals a complete mismatch to the data with a peak in September (Fig. 5), i.e. at the time when observational data show minimum numbers of egg-bearing shrimp.

Transition from SR I to SR II

In the stepwise update of model settings (from SR I) to SR II, the change to a spawning index based on a recent temperature dataset (scenario D.1) had only a minor effect on both the pattern and the absolute amount of landings and biomass (Fig. 6). When the

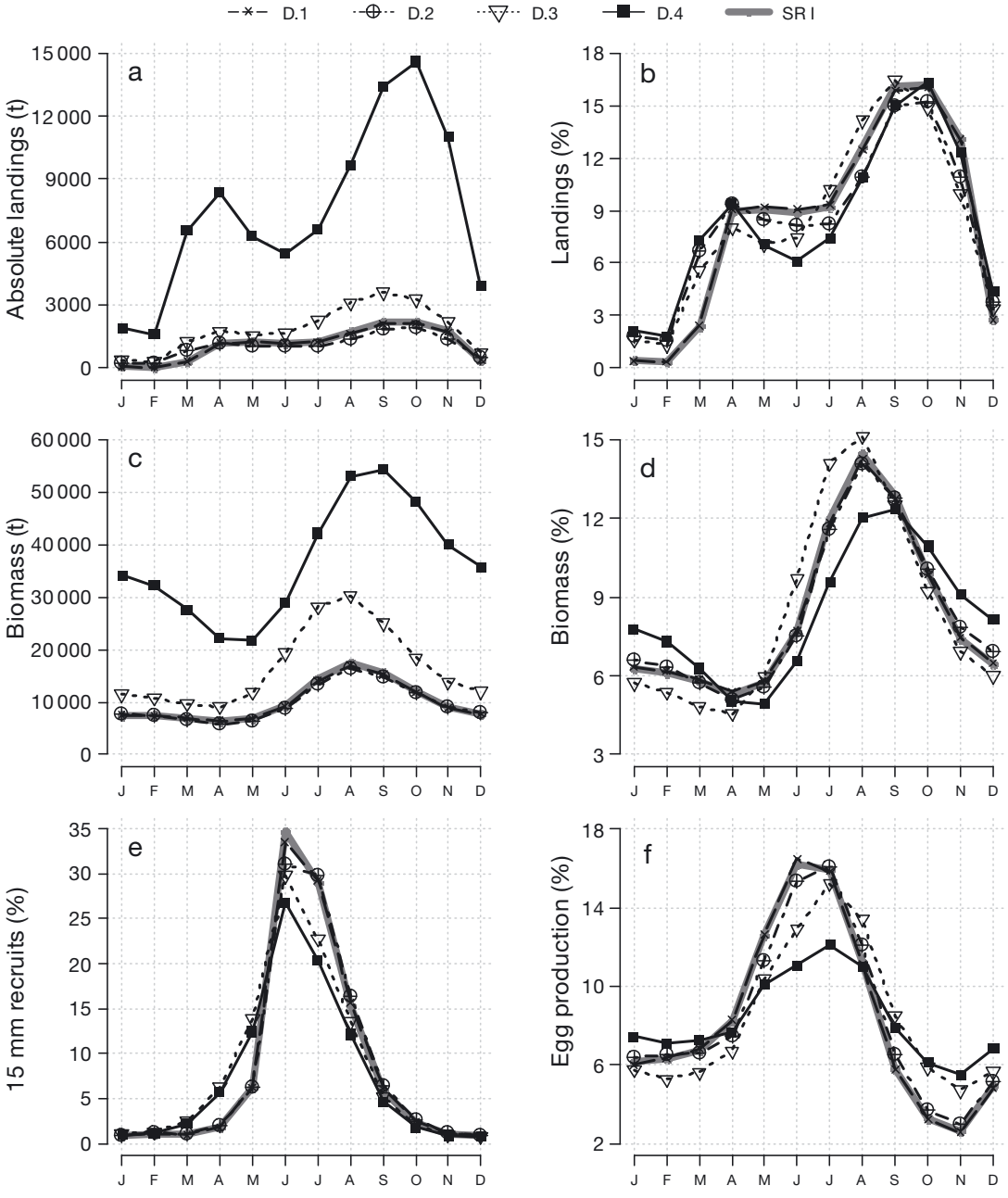

Fig. 6. Seasonal model outputs of (a,b) landings, (c,d) biomass, (e) 15 mm recruits and (f) egg production for the stepwise change (scenarios D.1–D.4) from the standard run (SR) I (old parameterization) to SR II settings (new parameterization). D.1: SR I with new spawning index; D.2: SR I with new spawning index and seasonal *F*; D.3: SR I with new spawning index, seasonal *F* and temperature; and D.4: SR I with new spawning index, seasonal *F*, temperature and *M*:*F* ratio. Scenario D.4 is equal to SR II except for the start number defining the size of cohorts starting each day into the model. t = tonne

fishing effort from the past decade (2002–2012) was also applied (scenario D.2), seasonal patterns of landings slightly changed with an increase in the first quarter of the year. The further implementation of recent (warmer) temperature data (scenario D.3) led to an overall increase in landings and biomass. Mean landings and biomass were about 30% higher compared with SR I. In terms of relative values (seasonal patterns), landings from March to June were slightly reduced compared with the autumn peak height. The increase in temperature led to a slight increase in recruits from April to May and a decrease in summer egg production accompanied by a shift of the peak from June to July. The strongest influence on both the seasonal and absolute amount of landings and biomass (Fig. 6) was induced by the change in the *M*:*F* ratio (scenario D.4). This resulted in a 6-fold increase of landings and a 3-fold increase of biomass. By inducing the recent *M*:*F* ratio representing the 2000s, the increase of relative landings in the first quarter was further strengthened in relation to scenario D.3. In addition, there was a slight decrease in relative landings from June to September. The peak in biomass is shifted from August to September with a lower relative biomass in summer and a higher biomass in winter compared with SR I. Applying the recent *M*:*F* ratio, the summer egg production was further reduced in relation to scenario D.3 and SR I leading to a more equally distributed egg production over the season.

The life cycle according to SR II

Similar to SR I, SR II is able to reproduce the observed patterns (r^2 = 0.89) in landings. SR II slightly overestimated landings in the first quarter and underestimated landings from May to July (Fig. 7a). The peak in autumn landings mainly (>50%) consisted of shrimps smaller than 60 mm length (Fig. 6i). In general, the share of larger shrimps (>60 mm) in the landings was higher in the first half of the year. The bulk of shrimps from autumn landings originated from winter eggs that started (hatched) during November of the previous year to June of the current year (Fig. 7e). Consequently, simulated peak landings mainly consisted of individuals that were younger than 1 yr. Shrimps caught in spring and early summer (April–July) were at least 1-yr old and originated mainly from spring and summer eggs of the previous year and to a smaller extent from winter eggs (produced 16–18 mo before catch). The biomass of the shrimp population peaked in August and was about 4 times higher in autumn than the simulated landings (Fig. 7j). In July and August, the biomass consisted of more than 50% of shrimps smaller than 50 mm. The observed size distribution of shrimp larger 50 mm (Fig. 8) sampled in September during the by-catch series and the Demersal Young Fish Survey was reproduced to a high degree by SR II (r^2 > 0.95). The peak in biomass was mainly produced by cohorts from summer eggs of the same year and by cohorts from winter eggs of the preceding winter (Fig. 7f). In contrast, the biomass in the first half of the year originates mainly from summer eggs of the preceding year.

SR II can reproduce the observed pattern in 15 mm recruits (r^2 = 0.98) with high accuracy (Fig. 6c). Most of the 15 mm recruits in June and July stem from eggs of the previous winter and spring of the same year (Fig. 6g,k). Thus, the June peak in recruits develops into the peak in biomass in August and finally becomes the peak in autumn landings. Egg production in SR II reproduced the input pattern of the spawning index (r^2 = 0.68); however, minima were overestimated leading to the underestimation of the height in the summer spawning peak (Fig. 7d). The total number of eggs produced in the model was more than 5 times higher than the number of eggs that started into the model (Fig. 7l). While the largest individuals represented just a small share of the total shrimp standing stock, they are extremely important for the reproduction of the population. During peak spawning in June, July and August, the largest females in the population (>70 mm) produce about 50% of the total egg amount despite their rather limited fraction of less than 10% of the population biomass. Summer egg-producing females are older than 1 yr and mainly

Fig. 7. Standard run (SR) II outputs for (a, e, i) landings, (b, f, j) biomass, (c, g, k) recruits and (d, h, l) egg production. (a–d) Relative seasonality of outputs together with observational data (for landings, recruits and egg production) and output data of SR I. (e–h) Temporal origin of outputs (landings, biomass, recruits and egg producers). Monthly results are displayed on the *x*-axis. On the *y*-axis, the whole simulation period is shown with the first year at the top and the last year at the bottom. The start month of each cohort contributing to the output is indicated by grey rectangles, whereby the colour intensity corresponds to the strength of the contribution in percent of the total monthly output (e.g. percentages of all monthly contributions sum up to 100 for January landings). (i–l) Absolute values of output data resolved by length classes of 10 mm; (l) length distribution of egg-producing females

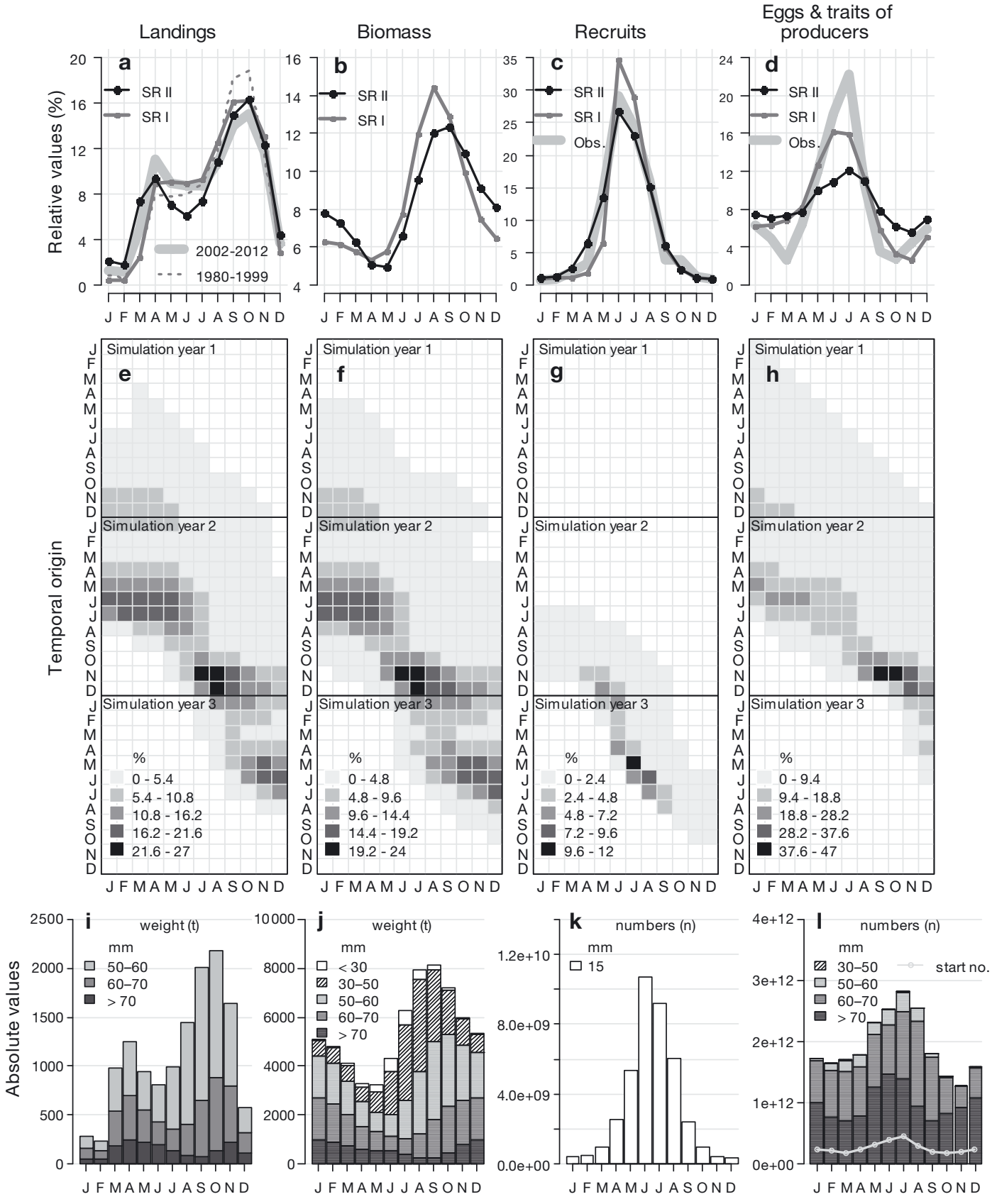
Landings
Biomass
Recruits
Eggs & traits of producers
a
b
c
d
SR II
SR I
Obs.
2002-2012
1980-1999
Relative values (%)
J F M A M J J A S O N D
Temporal origin
Simulation year 1
Simulation year 2
Simulation year 3
e
f
g
h
%
0 - 5.4
5.4 - 10.8
10.8 - 16.2
16.2 - 21.6
21.6 - 27
0 - 4.8
4.8 - 9.6
9.6 - 14.4
14.4 - 19.2
19.2 - 24
0 - 2.4
2.4 - 4.8
4.8 - 7.2
7.2 - 9.6
9.6 - 12
0 - 9.4
9.4 - 18.8
18.8 - 28.2
28.2 - 37.6
37.6 - 47
Absolute values
i
weight (t)
j
weight (t)
k
numbers (n)
l
numbers (n)
mm
50–60
60–70
> 70
< 30
30–50
15
start no.

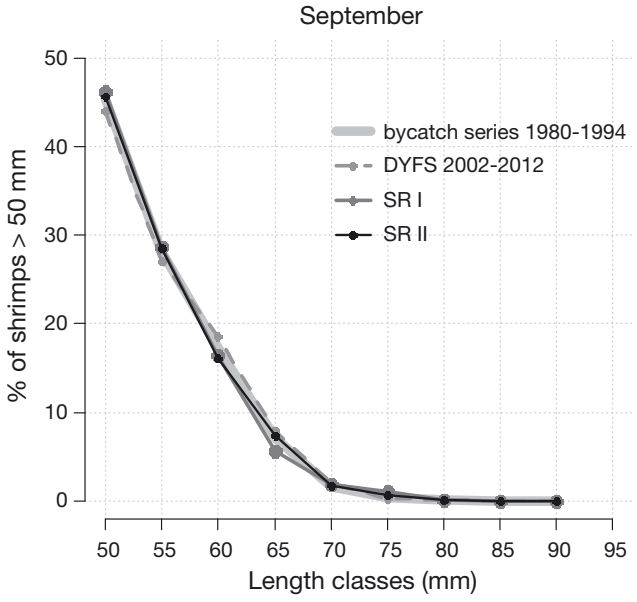

Fig. 8. Simulated and observed length-frequency distributions of the population in September aggregated by 5 mm length classes. DYFS: Demersal Young Fish Survey after Siegel et al. (2008); by-catch series after Tiews (1990)

stem from summer eggs (Fig. 7h). Winter and spring eggs were mainly produced by females stemming from winter eggs.

The length-frequency distribution in June was dominated by individuals <30 mm (Fig. 9). In July and August, this 'summer' cohort was growing and individuals started to enter the fishery at a length >50 mm in August and September. In the following months until May of the next year, length-frequency distributions exhibited a peak at a length of 50 mm, which was induced by the fishery harvesting mainly the summer cohort. The number of larger individuals decreases steadily from October to May. When the new 'summer' cohort in June appeared, there were only few large (>60 mm) individuals left. Females became larger than males according to their higher growth rate, which involves a lower cumulative mortality over their lifetime. Due to this selective mortality of males, most individuals larger 60 mm were females.

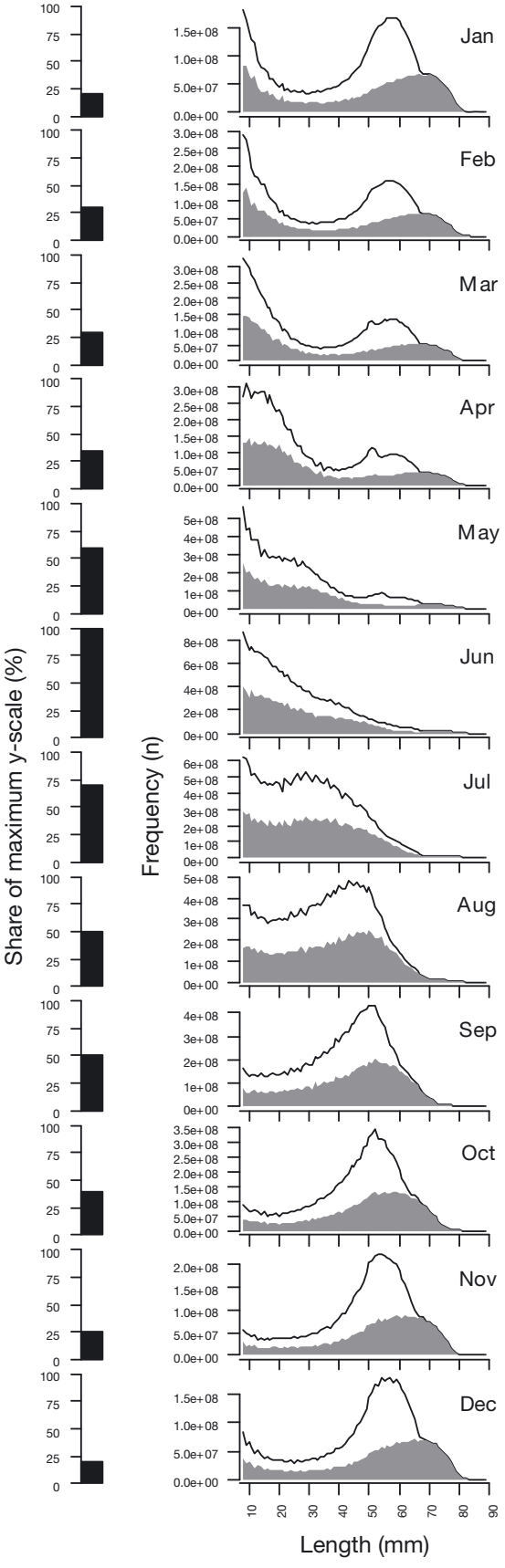

Fig. 9. Population length-frequency distribution on the 15th of each month according to standard run (SR) II. In the right panels, the upper black line indicates the frequency of both sexes and the white and grey areas the number of males and females, respectively. Left panels (black bars) indicate the different scales of the *y*-axes in relation to the largest scale occurring in June

DISCUSSION

Growth

Growth and mortality are the 2 dominant processes determining shrimp population dynamics. Since growth rates are generally very difficult to determine in crustaceans, it is not surprising that diverging views exist in the literature varying from low growth rates (e.g. Labat 1977, Oh et al. 2001, Campos et al. 2009) to high growth rates (Meixner 1969, Tetard 1985, Hufnagl & Temming 2011b). Different views on the growth rates are closely related to different understandings of the life cycle. Promoters of slow growth relate the main seasonal peak in landings (autumn) to the egg production of the previous summer (Campos et al. 2009), while faster growth rates are required to relate it to the winter egg production (Kuipers & Dapper 1984) or even the summer egg production of the same year (Boddeke & Becker 1979). The life cycle model presented here offers an opportunity to check the growth-rate assumptions based on their ability to reproduce the observed seasonal patterns in the observational data. With low growth rates, as predicted e.g. by Eq. (6) from Kuipers & Dapper (1984), neither the observed pattern of seasonal catches nor the seasonal pattern of egg production and the length compositions can be correctly predicted. We can therefore conclude that these low growth rates cannot be representative of the wild population, especially not for the female part, which is mostly responsible for the landings peak in autumn. In case of the Kuipers & Dapper's (1984) equation, the low growth rates reflect a mean situation for both sexes, since these were not separated in the original data by M. Fonds (pers. comm.). More recent experiments with sex differentiation (Hufnagl & Temming 2011a) and a synthesis of all available growth data (Hufnagl & Temming 2011b) confirm the repeated observation of high growth rates and generally significantly higher female growth rates.

The latter study (Hufnagl & Temming 2011b) also revealed a substantial amount of variability in the growth data, especially between different datasets, which justifies the implementation of a certain level of growth variability into the model (here a standard deviation of 30% was used). In earlier model versions, the variability was linked to the catabolic term of the growth equation only. This, however, had the unwanted effect of generating a certain number of very large shrimp in the simulation, which have not been observed in any of the surveys. The implementation chosen here attaches the variability to the complete equation, which has the effect of more variation in medium length classes and less variation in length classes close to the asymptotic length. The effect of this change on the aggregated outputs, however, was only marginal (not shown here).

The choice of the growth Eq. (6) from Kuipers & Dapper (1984) had a clear influence on the generated results. We achieved a better fit to the combined length growth data if we introduced a second temperature effect in the catabolic term of the equation (see Eq. 8 and Hufnagl & Temming 2011b). This second temperature term represented an interaction effect between length and temperature, leading to smaller increases of growth rates of larger shrimp at higher temperatures. This length temperature interaction led to a reduced summer egg production. The reason is that the egg numbers increase exponentially with shrimp length and consequently large shrimp size classes in summer contribute substantially to the total summer egg production (see Fig. 7l).

Mortality

Overall, the simulated seasonal patterns are not very sensitive to the actual mortality levels (Z) or to the slope of the mortality size relation (results not presented here). Total mortality estimates used here are in the range of observations by other authors: higher values have been reported by Viegas et al. (2007) with Z = 8.7–10.9 yr^{-1} and Kuipers & Dapper (1981) with Z = 7.7–9.3 yr^{-1}; lower values were found by Henderson et al. (2006) with Z = 2.92 yr^{-1} and Oh et al. (1999) with Z = 3.96 yr^{-1}. However, the differences partly reflect differences in methodology with the very high estimates being derived from estimates of production over mean biomass based on Allen (1971). The lower estimates refer to basically unfished areas and hence reflect only natural mortality. Additional problems in such estimates originate from a restricted depth range sampled in combination with seasonal emigration of larger shrimp into deeper, unsampled areas (Oh et al. 1999, Viegas et al. 2007). Our estimates are based on size distributions from spatially extensive sampling programs covering a wide depth range (Hufnagl et al. 2010b) and should therefore be robust against the emigration bias. Nevertheless, due to the large mesh size, only shrimps <45 mm were represented. Studies applying length-based methods (e.g. Oh et al. 1999), such as length-converted catch curves (Pauly 1983), to species with strong seasonality in growth and recruitment are furthermore subject to a methodological bias (Hufnagl

et al. 2013). Hufnagl et al. (2010b) have investigated this bias in *Crangon crangon*-specific simulation studies and derived a bias correction function to correct raw estimates for the resulting underestimation of total mortality.

The critical aspect in our simulation is the assumed seasonal variation of mortality. With size-specific natural mortalities constant in all months, it was impossible to reproduce any of the field datasets (Fig. 5). A central result from the model exercise is therefore that mortalities acting on all life stages of *C. crangon* must differ substantially between seasons. The main effect of constant mortalities was that the relative recruitment contribution of the winter egg production disappeared almost completely because the long development times of eggs and larvae resulted in very high cumulative mortalities, when compared with the situation for the summer egg production. However, since the main recruitment signal of 15 mm-sized shrimps in coastal regions could clearly be related to the winter egg production (Temming & Damm 2002), the constant mortality scenario is incompatible with the observational data.

The allocation of monthly mortality values for the younger stages was done in a rather heuristic way, basically following the seasonal temperature curve. For juveniles and adults, highest mortalities were set in months with observed maximum densities of relevant predators. While this reflects our best understanding of the seasonality of predation, maximum consumption is not necessarily equivalent to the maximum mortality, since mortality was defined by the consumption over mean biomass in the interval considered. This aspect has not been investigated in detail, because only very limited data exist with regard to shrimp densities and numbers consumed covering all size classes, the entire year and depth range of their distribution area.

Recruitment pattern

In the previous model versions, 4 different temperature datasets were used, referring to inshore and offshore locations on the German and the Dutch coasts, respectively. The larvae were allocated to the warmer of the 2 regions at any time. The reason for this was that with only German temperatures, the previous versions were unable to generate a recruitment peak of 15 mm juveniles in May–June. The inclusion of Dutch water temperatures was sufficient to make the simulations match with the observational data from the German as well as from the Dutch tidal flats (Beukema 1992, Temming & Damm 2002). Such a match was an essential precondition for the further application of the model to predict the seasonal patterns of other life stages. However, detailed analysis of the likelihood and the dimension of a hypothetical import of larvae from Dutch waters into German coastal regions revealed that while this import via passive drift is actually quite likely (Daewel et al. 2011), the numerical contributions decrease rapidly with increasing distance from the target region if vertical migration patterns are considered (Hufnagl et al. 2014). Hence, we decided not to use the Dutch temperature data but to allow instead for a stronger individual variability around the mean values of the experimentally determined stage duration times. This variability was adjusted to the same level that was also used in growth variability of juvenile and adult shrimp. This measure had the same effect as the Dutch water temperatures, namely producing a strong increase of 15 mm juveniles in May–June with a peak in June.

The majority of the 15 mm recruits in May and June originate from eggs of the previous winter egg production as suggested by Kuipers & Dapper (1984) and later confirmed by Temming & Damm (2002). However, with the higher degree of developmental and growth variability implemented here, slower-growing cohorts of the previous summer also provide a smaller contribution. Furthermore the second half of the recruitment peak receives contributions from fast-growing cohorts of the early summer of the same year. In essence, with a higher degree of variability implemented, the explanations of Campos et al. (2009) and Boddeke & Becker (1979) are also partly true, although they do not explain the main event correctly. All contributions from 2 summer egg production periods and the winter egg production end up in a unimodal peak of recruits, because the early contributions are delayed by the winter temperature, while the late contributions are accelerated by high summer temperatures.

Catch rates

If the observed recruitment peak of 15 mm shrimp is matched in the simulations, the seasonal pattern of commercial landings can be reproduced well in the model runs. The main peak in autumn follows the recruitment peak with a delay of 3 mo and the initial increase in August originates mostly from the winter egg production with minor contributions from the 2 summer periods. Later in the season the contribution of the same year's summer period increases and then

dominates the catches in the subsequent spring and early summer.

In the years 1980–1999, the patterns of spring and early summer catches are rather stable, which is also reproduced in the simulations of SR I, while in the subsequent decades, landings decrease somewhat after the small April peak. This pattern is also visible in the simulations, but somewhat exaggerated in SR II. The height of the April peak in relation to the autumn peak and the catch levels in May–July depend largely on the total mortality level during autumn and winter. Rückert (2011) has investigated this in detail and confirmed the decrease of the spring landings with increasing fishing intensity and constant predation mortality.

The remaining deviations between simulation and observation may originate from the use of the seasonal effort pattern as a template for the seasonal fishing mortality pattern. This implies that there are no seasonal differences in catchability. However, shrimp distribute over a wider area of deeper waters during winter and their activity levels may be reduced at low temperatures (Reiser et al. 2014), while the gear operation in more turbulent waters may also contribute to lower catchability; hence, catchability is most likely reduced in winter months, which may explain our overestimation of winter catches. In contrast, in summer, shrimps move closer to the coast and become more active, which may lead to higher catchabilities.

Egg production

The current implementation of maturation and egg production needs refinement. At present, a mean yearly pattern of the share of egg-bearing females per length class is used. The maturation data used here originated from the by-catch sampling program described in Tiews (1990) and were based on the share of egg-carrying females in relation to all females as a proxy for maturation. In these average data, the maximum share of egg-carrying females did not exceed 60%, but this share could be as high as 100% for large shrimp in some months (Siegel et al. 2008). However, the effects of a lower overall share of mature females on the results were limited, since this implies that a constant part of the modelled female population does not participate in spawning, which had no effect on the seasonal patterns.

The seasonal pattern of egg production — as derived from observational data before 1990 — was characterised by a dominant summer peak in July followed by a minimum in September–October and a smaller winter peak. The simulations of both SR I and SR II are able to reproduce this principal pattern, but the pattern is less pronounced than the observed one, especially in SR II. While a pronounced summer peak can be confirmed with independent data on seasonal larval abundances (Kühl & Mann 1963, Wehrtmann 1989), the model prediction of a secondary larval peak in March–April originating from winter eggs was more difficult to verify. The only confirmation besides the presence of egg-bearing females in winter can be found in Rees (1952), which showed the highest abundances of *C. crangon* larvae in January, March and April in aggregated continuous plankton recorder data of all North Sea tracks in 1947–1949. However, the model could support the planning of a targeted survey by predicting the time window of larval occurrence, and this information could be combined with recent information of the winter distribution of egg-carrying females (Schulte 2015) and coastal water drift patterns (Hufnagl et al. 2014).

The large summer peak originated as offspring from large shrimp of the previous year, which resume growth and egg release with increasing spring temperatures. Since the number of eggs per female increased by a power of 3 with body length, these large shrimp produced very high numbers of eggs per female. Due to the high temperatures, the intermoult periods were also short, with the consequence that each female produced eggs at a higher frequency. These effects together generated the dominant summer peak. The application of the growth model with a temperature effect in the catabolic term (Eq. 8) restricted the temperature-dependent growth of large shrimp and reduced the summer peak considerably, when compared with the results of a growth model lacking an interaction term between length and temperature.

The winter peak was supported by larger numbers of adult shrimp of the new incoming cohort, which also formed the basis of the autumn peak in commercial catches. However, these shrimp were smaller and younger than those generating the summer peak, and due to the low winter temperatures, intermoult periods and egg development were considerably prolonged.

The very low numbers of egg-bearing shrimp in September and October could only be reproduced in the simulations if a minimum age at maturity was introduced. Since in the current model the implementation of maturity was size dependent and hence coupled to growth, the fast growth of the incoming new cohort led inevitably also to maturation at young ages with subsequent egg production. Therefore,

without a minimum spawning age, increasing egg production was predicted for September with maximum values for October and November, which contradicts the observations (Fig. 5c, scenario C2).

The optimal fit to the observed data was achieved with a minimum age of 180 d calculated from the start of the juvenile stage with a length of 6 mm. Siegel et al. (2008) observed a shift in the maturity between winter and spring, with a smaller length at 50% maturity in spring (55.4 mm in contrast to 62 mm). This would be compatible with the idea of a minimum spawning age, which would shift maturity to larger sizes in the comparatively younger shrimp which dominate in winter. Such a pattern can actually be seen in Fig. 7l, where in November and December the class of the largest shrimps (>70 mm) dominated among the egg-producing size classes, while the next smaller length class (60–70 mm) contributed only half as many egg-producing females. In spring, these relationships were reversed and the contribution of the next smallest size class also becomes visible. An alternative mechanism could be a hormone-controlled suppression of maturation at this time of the year (Klęk-Kawińska & Bomirski 1975), which may be triggered through day length. This would be even easier to implement in the simulation model and the results would obviously match the observations.

However, a hypothetical minimum age at first maturity has the additional advantage of being able to explain the regional shifts in the months with minimum numbers of egg-bearing females in Danish and British waters as a result of differences in temperature-dependent growth and recruitment patterns (Rückert 2011). If these differences were to be explained by hormonal controls triggered by day length, then the local populations would have to differ genetically in these trigger values.

Overall, the simulated egg production was significantly (up to 5 times) higher than the numbers of the respective run that were used to generate the cohorts of spawning females. This discrepancy could be explained in a number of ways. The most obvious was related to the open boundaries of the North Sea coastal ecosystem inhabited by *C. crangon*. Large amounts of larvae can be exported with the residual currents into northern regions, including the Skagerrak (Daewel et al. 2011, Hufnagl et al. 2014). Alternatively, our egg and larval mortalities may be underestimated or the moulting frequencies of the females are overestimated. There are indications of egg loss during the egg-carrying phase (Oh & Hartnoll 2004) but the magnitude of this loss (10–17%) is too small to explain the large discrepancy.

Size compositions

The aggregated size composition of adult shrimp (>50 mm) of the simulated cohorts closely matched the observed one (Fig. 8). This is, however, not a truly independent check, since the observed size compositions were used together with the laboratory-derived growth rates to estimate the level of total mortality (Hufnagl et al. 2010b). Since these mortality levels were used in the simulations, there is a certain degree of circularity in this comparison. However, the match can serve as a check for internal consistency of this fairly complex simulation exercise.

The seasonal pattern of the adult shrimp population can be described as one major cohort wave that shifts to larger length classes with time. The recruitment peak from the winter egg production was immediately followed by the rapidly developing cohorts from spring and early summer eggs. Together, these form a major wave of adult shrimp, which was visible as a peak in the size distribution from July to May of the subsequent year. At the time when peak biomass (August) or peak landings (September–October) occur, hardly any shrimp older than 12 mo (after settlement) are left, so that in essence the whole population is exchanged. This pattern emerges from the rapid acceleration of cohort development and growth with increasing spring temperatures, which leads to an increasing overlap of the summer and winter cohorts in combination with high mortality levels in summer and autumn. The shrimp from this combined winter and early summer egg production formed the basis for the fishery in the autumn of the same year, as well as the following winter and spring. This explained why a complete failure of the fishery in autumn, as experienced in 1983 and 1990 is generally followed by a failure of the subsequent spring fishery (ICES 2014) as well.

The simulation provided size distributions for the entire size range (6–80 mm); however, very few data exist to compare the results with because in most surveys only catch sizes above 45 mm are sampled quantitatively. This is also due to the fact that a representative sampling with a standard gear of all size classes in all depth strata is almost impossible. The simulated overall size distributions revealed 3 different patterns: bimodal distributions can be seen in winter (December–April), when part of the new cohort forms a peak between 10 and 30 mm; in late spring and early summer the distribution resembled a single falling slope with maximum numbers in the smallest size classes; in autumn the pattern was rather unimodal. The existence of the small peak in

the bimodal patterns in winter has been confirmed by field sampling programs covering the winter months: there, a peak was observed in the length class 10–20 mm in push-net catches in January and February (Del Norte-Campos & Temming 1998) and likewise in November (Jansen 2002). Jansen (2002) also presented length-frequency distributions from combined catches of push-nets and 2 m beam trawls conducted in deeper waters, which confirm the bimodal pattern in April and May with peaks in the range 10–20 and 30–50 mm.

Interlocking of cohorts

The winter egg production of a given year (X) originates mainly from cohorts that start as eggs also in winter, e.g. the egg production of December is related mainly to cohorts generated between November (X − 1) and February (X) with small contributions also from April to June (X). For late winter, the pattern is somewhat shifted, e.g. the eggs spawned in February of year X are from cohorts that start either in November–December in year X − 2 or between April and June and even July of year X − 1. The peak of summer egg production in August (X) is linked to cohorts that start between June and September (X − 1) with minor contributions of even November (X − 1). Due to the variability of growth and development rates, these relations are not rigid and there is a certain amount of exchange between the 2 cohorts, as can be seen in the large number of months that deliver minor contributions to each of the seasons. Hence, if growth conditions in the field are good between late summer and winter, then cohorts from the early summer egg production can make a stronger contribution to spawning in the subsequent winter. However, if mortality in winter and spring is low, then cohorts originating from winter eggs could not only produce eggs in the subsequent winter but also continue to spawn into the following summer. Given their large size attained by then and the exponential relation of fecundity with length, these cohorts will contribute substantially to the egg production.

Temperature changes

The computed results should not be over interpreted with regard to their biological significance given the lack of information on effects of temperature on other ecosystem components, such as prey production or predation. The simple overall effect of warmer temperatures in the current growth parameterisation is higher growth rates, which translates into more biomass, catch and egg production. But such effects will only occur if food supply increases in the same manner and without any changes in mortality. These results are hence not discussed here any further. Another aspect was related to the effect of temperature on development times of eggs and larvae, which would translate into overall shorter development times. The overall effects on the seasonal patterns, however, were rather minor.

Changes in the *F*:*M* ratio

The most pronounced effects that resulted from changes in the parameterisation of the model for different decadal periods related to the changes in the *F*:*M* ratio. Clearly, a lower *M* will have direct positive effects on landings biomass and egg production. In our model implementation, the natural mortality of juvenile shrimp was coupled to the level of the adult shrimp as mortality was interpolated between adult and larval shrimps assuming an exponential decrease. This has the side effect that a decreasing *M* of the adults also reduced the *M* of the juvenile shrimp, which translated into larger numbers of recruits entering into the fishery. This exaggerates the mere effect originating from lower *M* in the fished size classes. This implementation was, however, in principle, biologically meaningful because the main predators of adult shrimp (cod and whiting) were also the main predators of juvenile shrimp (Welleman & Daan 2001, Jansen 2002, Temming & Hufnagl 2015).

Additional effects were related to the different seasonality of both mortality components: while the fishing mortality was assumed to follow the pattern of fishing effort—which is rather stable between April and November—the natural mortality varied strongly between seasons. Hence, if mortality was shifted from *M* to *F*, the total mortality of juvenile and adult shrimp in summer and autumn decreased, which especially benefited the overwintering cohorts and led to higher catches, biomass and egg production in winter and spring.

Comparison with other modelling approaches for shrimp populations

Population modelling of shrimp species is most widespread for the taxonomic groups of pandalids (e.g. Gallagher et al. 2004) and penaeids (e.g. Cail-

louet et al. 2008, Punt et al. 2011). In pandalid species, the life cycle is more complex due to potandric hermaphroditism, but since these are longer lived and often ageing is possible, conventional age-based analytical methods are frequently applied (Fox 1973, Gallagher et al. 2004). In penaeid populations, the situation is different and more similar to *C. crangon*: most species are short lived and seasonal growth variations and multiple recruitment waves have to be taken into account (e.g. Ye 1998). Yet, many applications combine estimates of seasonal juvenile and adult growth rates from monthly samples of length-frequency distributions with length-based estimations of total mortality, which are subsequently used to estimate the maximum yield per recruit as a function of fishing mortality (Gallagher et al. 2004) or opening month of the fishery (Ye 1998).

Punt et al. (2010) have developed a fairly advanced size-based model that uses size-structured survival and size-transition matrices to model the population structure in weekly time steps of 3 peneaid species that are caught in a mixed fishery in Northern Australia. The computationally demanding model includes an economic component and can actually estimate a number of biological parameters, such as growth and selectivity, together with the effort patterns to maximize profits while being fitted to time series of size structure and catch. Such models could theoretically include more biological detail, e.g. seasonally variable mortalities or growth rates, but often sufficiently detailed biological data are not available for a parameterization.

An interesting modelling study of an unfished crangonid species was presented by Labat (1991a,b). The aim was—similar to our approach—to model the complete life cycle, including the seasonally changing population structure. Labat adopted the simulation model of Hampton & Majkowski (1987), which was designed to create artificial catch composition data with known parameters as a test tool for statistical methods estimating growth and mortality parameters from length-composition data of catches of fished species. That model calculates for large numbers of individuals the point in time when an individual dies (either through fishing or natural mortality) using random numbers and inverted probability density functions. Subsequently, the size of each dead individual is calculated from a Bertalanffy function including seasonality, leading to monthly aggregated size distributions of catches. Labat (1991a,b) modified this approach to simulate the dynamics of the size structure of an unfished shrimp population (*Philocheras trispinosus*). He calculated in daily time steps to also model the stock numbers, maturation and egg production. Both approaches use an integrated seasonal version of the Bertalanffy growth function and constant mortalities. Our own approach can be viewed as a further advancement in the direction of increasing complexity of the simulated life cycle. We have added temperature-dependent development of larvae and size- and season-specific mortalities. An important improvement is our growth model, which was implemented as a flexible differential equation to account for the interaction of size and temperature on growth and egg production rates.

CONCLUSION

With regard to the life cycle of brown shrimp we were able to do the following:

(1) solve the debate about the reproduction period contributing most to the commercial fishery peak and subsequent spawning in favour of the winter egg production;

(2) provide strong evidence for fast growth rates because, in combination with the given mortality levels, the slow growth assumption in the simulations leads to seasonal patterns contradicting the observed ones;

(3) show that natural mortality of the early pelagic stages must exhibit a pronounced seasonality;

(4) test an alternative explanation for the lack of egg-bearing shrimp in September–October based on a minimum spawning age and the transition of cohorts;

(5) describe the population structure as a single seasonal wave pattern with early and dominant contributions originating from winter egg production followed immediately by contributions from the summer egg productions and;

(6) show that summer egg production is mostly performed by large females originating from the previous summer while the winter egg production is mostly related to younger females from the previous winter. With higher variability in development and growth rates, both cohorts become increasingly interlocked.

Our model framework has successfully integrated complex life cycle processes into a yield-per-recruit-type assessment model. Partly, this was only possible due to the enormous increase in computing power that has happened since the end of the 1990s. The main application for this new tool is the optimization of the yield per recruit of the currently unmanaged

Crangon crangon fishery in the frame of the fisheries self-management under the ongoing marine stewardship council certification.

Our model framework is generally applicable to short-lived species with pronounced seasonal dynamics, whether in relation to multiple cohorts or variations in growth and mortality rates. This refers likewise to invertebrate species in temperate and tropical climates, and also to many fish species in tropical waters. This framework can be applied to not only clarify the life cycle in a quantitative way or at least to identify gaps in the quantitative understanding of processes, but also guide management decisions in harvested species, such as mesh size changes, closed seasons or generally seasonal varying effort patterns.

Acknowledgements. The study was financially supported by the projects COEXIST (KBBE-3-245178-COEXIST), VECTORS (Vectors of Change in Oceans and Seas Marine Life, EU FP7, 266445), and CRANNET (Optimierte Netz-Steerte für eine ökologisch und ökonomisch nachhaltige Garnelenfischerei in der Nordsee). Furthermore, the German Federal Ministry of Food and Agriculture (BMEL) funded substantial parts of the work (project 03HS030). We thank the 'Landesbetrieb für Küstenschutz, Nationalpark und Meeresschutz Schleswig-Holstein' (LKN) for providing daily temperature data from Büsum, and the 'Bundesamt für Hydrographie' for providing temperature time series from the North Sea MARNET stations. Finally, we thank our 3 referees for their constructive and thorough review, which has clearly helped to improve our manuscript.

LITERATURE CITED

Allen KR (1971) Relation between production and biomass. J Fish Res Board Can 28:1573–1581

Beukema JJ (1992) Dynamics of juvenile shrimp *Crangon crangon* in a tidal-flat nursery of the Wadden Sea after mild and cold winters. Mar Ecol Prog Ser 83:157–165

Beukema JJ, Dekker R (2014) Variability in predator abundance links winter temperatures and bivalve recruitment: correlative evidence from long-term data in a tidal flat. Mar Ecol Prog Ser 513:1–15

Beverton RJH, Holt SJ (1957) On the dynamics of exploited fish populations. Her Majesty's Stationery Office, London

Boddeke R, Becker HB (1979) A quantitative study of the stock of brown shrimp (*Crangon crangon*) along the coast of the Netherlands. Rapp P-V Reun Cons Int Explor Mer 175:253–258

Cadrin SX, Boutillier JA, Idoine JS (2004) A hierarchical approach to determining reference points for Pandalid shrimp. Can J Fish Aquat Sci 61:1373–1391

Caillouet CW Jr, Hart RA, Nance JM (2008) Growth overfishing in the brown shrimp fishery of Texas, Louisiana, and adjoining Gulf of Mexico EEZ. Fish Res 92:289–302

Campos J, Van der Veer HW, Freitas V, Kooijman SALM (2009) Contribution of different generations of the brown shrimp *Crangon crangon* (L.) in the Dutch Wadden Sea to commercial fisheries: a dynamic energy budget approach. J Sea Res 62:106–113

Criales MM, Anger K (1986) Experimental studies on the larval development of the shrimps *Crangon crangon* and *C. allmanni*. Helgol Meeresunters 40:241–265

Daewel U, Schrum C, Temming A (2011) Towards a more complete understanding of the life cycle of brown shrimp (*Crangon crangon*): modelling passive larvae and juvenile transport in combination with physically forced vertical juvenile migration. Fish Oceanogr 20:479–496

Dänhardt A (2010) The spatial and temporal link between common terns *Sterna hirundo* and their prey fish in the Wadden Sea. PhD dissertation, University of Oldenburg & Institute of Avian Research, Wilhelmshaven

Del Norte-Campos AGC, Temming A (1998) Population dynamics of the brown shrimp *Crangon crangon* L., in shallow areas of the German Wadden Sea. Fish Manag Ecol 5:303–322

Feller RJ (2006) Weak meiofaunal trophic linkages in *Crangon crangon* and *Carcinus maenus*. J Exp Mar Biol Ecol 330:274–283

Fonds M (1978) The seasonal distribution of some fish species in the Western Dutch Wadden Sea. In: Dankers N, Wolff WJ, Zijlstra JJ (eds) Fishes and Fisheries of the Wadden Sea. Report no. 5 of the Wadden Sea Working Group. Stichting Veth tot Steun aan Waddmonderzoek, Leiden, p 42–77

Fox JRWW (1973) A general life history exploited population simulator with Pandalid shrimp as an example. Fish Bull 71:1019–1028

Gallagher CM, Hannah RW, Sylvia G (2004) A comparison of yield per recruit and revenue per recruit models for the Oregon ocean shrimp, *Pandalus jordani*, fishery. Fish Res 66:71–84

Greve W, Reiners F (1988) Plankton time-space dynamics in German Bight — a systems approach. Oecologia 77: 487–496

Hampton J, Majkowski J (1987) A simulation model for generating catch length-frequency data. In: Pauly D, Morgan GR (eds) Length-based methods in fisheries research. ICLARM, Safat, p 193–202

Havinga B (1930) Der Granat (*Crangon vulgaris* Fabr.) in den holländischen Gewässern. J Cons Cons Int Explor Mer 5:57–87

Henderson PA, Seaby RM, Somes JR (2006) A 25-year study of climatic and density-dependent population regulation of common shrimp *Crangon crangon* (Crustacea: Caridea) in the Bristol Channel. J Mar Biol Assoc UK 86: 287–298

Hufnagl M, Temming A (2011a) Growth in the brown shrimp *Crangon crangon*. I. Effects of food, temperature, size, gender, moulting, and cohort. Mar Ecol Prog Ser 435:141–154

Hufnagl M, Temming A (2011b) Growth in the brown shrimp *Crangon crangon*. II. Meta-analysis and modelling. Mar Ecol Prog Ser 435:155–172

Hufnagl M, Temming A, Danhardt A, Perger R (2010a) Is *Crangon crangon* (L. 1758, Decapoda, Caridea) food limited in the Wadden Sea? J Sea Res 64:386–400

Hufnagl M, Temming A, Siegel V, Tulp I, Bolle L (2010b) Estimating total mortality and asymptotic length of *Crangon crangon* between 1955 and 2006. ICES J Mar Sci 67: 875–884

Hufnagl M, Huebert KB, Temming A (2013) How does seasonal variability in growth, recruitment, and mortality

affect the performance of length-based mortality and asymptotic length estimates in aquatic resources? ICES J Mar Sci 70:329–341

Hufnagl M, Temming A, Pohlmann T (2014) The missing link: tidal-influenced activity a likely candidate to close the migration triangle in brown shrimp *Crangon crangon* (Crustacea, Decapoda). Fish Oceanogr 23:242–257

ICES (International Council for the Exploration of the Sea) (2003) Report of the Working Group on *Crangon* Fisheries and Life History (WGCRAN). ICES CM 2003/G:01

ICES (International Council for the Exploration of the Sea) (2006) Report of the Working Group on *Crangon* Fisheries and Life History (WGCRAN). ICES CM 2006/LRC: 10

ICES (International Council for the Exploration of the Sea) (2013) Report of the Working Group on *Crangon* Fisheries and Life History (WGCRAN). ICES CM 2013/ SSGEF:12

ICES (International Council for the Exploration of the Sea) (2014) Report of the Working Group on *Crangon* Fisheries and Life History (WGCRAN). ICES CM 2014/ SSGEF:08

Jansen S (2002) Das Räuber-Beutesystem juveniler Gadiden, Grundeln und Garnelen im Wattenmeer nördlich von Sylt. PhD dissertation, University of Hamburg

Kłęk-Kawińska E, Bomirski A (1975) Ovary-inhibiting hormone activity in shrimp (*Crangon crangon*) eyestalks during the annual reproductive cycle. Gen Comp Endocrinol 25:9–13

Kühl H, Mann H (1963) On the distribution of shrimp larvae (*Crangon crangon* L.) in the estuary of the Elbe. Veröff Inst Küst Binnenfisch 50–52

Kuipers BR, Dapper R (1981) Production of *Crangon crangon* in the tidal zone of the Dutch Wadden Sea. Neth J Sea Res 15:33–53

Kuipers BR, Dapper R (1984) Nursery function of Wadden Sea tidal flats for the brown shrimp *Crangon crangon*. Mar Ecol Prog Ser 17:171–181

Labat JP (1977) Ecology of *Crangon crangon* (L.) (Decapoda Carida) in a lagoon of the coast of the Languedoc. Vie Milieu 27:359–367

Labat JP (1991a) Model of a shrimp population (*Philocheras trispinosus*) II. Simulation of the energy fluxes. Ecol Modell 53:95–107

Labat JP (1991b) Model of a shrimp population (*Philocheras trispinosus*) I. Simulation of the size structure. Ecol Modell 53:75–93

Martens E, Redant F (1986) Protandric hermaphroditism in the brown shrimp, *Crangon crangon* (L.) and its effect on recruitment and reproductive potential. ICES CM K: 37

Megrey BA, Hinckley S (2001) Effect of turbulence on feeding of larval fishes: a sensitivity analysis using an individual-based model. ICES J Mar Sci 58:1015–1029

Meixner R (1969) Wachstum, Häutung, und Fortpflanzung von *Crangon crangon* (L.) bei Einzelaufzucht. Ber Dtsch Wiss Komm Meeresforsch 20:93–111

Neudecker T, Damm U (1992) Seasonality of egg-bearing shrimp (*Crangon crangon* L.) in coastal waters of the German Bight. ICES CM K: 28

Oh CW, Hartnoll RG (2004) Reproductive biology of the common shrimp *Crangon crangon* (Decapoda: Crangonidae) in the central Irish Sea. Mar Biol 144:303–316

Oh CW, Hartnoll RG, Nash RDM (1999) Population dynamics of the common shrimp, *Crangon crangon* (L.), in Port Erin Bay, Isle of Man, Irish Sea. ICES J Mar Sci 56: 718–733

Oh CW, Hartnoll RG, Nash RDM (2001) Feeding ecology of the common shrimp *Crangon crangon* in Port Erin Bay, Isle of Man, Irish Sea. Mar Ecol Prog Ser 214:211–223

Pauly D (1983) Length-converted catch curves: a powerful tool for fisheries research in the tropics (part I). Fishbyte 1:9–13

Pauly D (1998) Beyond our original horizons: the tropicalization of Beverton and Holt. Rev Fish Biol Fish 8:307–334

Peterson I, Wroblewski JS (1984) Mortality-rate of fishes in the pelagic ecosystem. Can J Fish Aquat Sci 41: 1117–1120

Plagmann J (1939) Ernährungsbiologie der Garnele *Crangon vulgaris* Fabr. Helgol Meeresunters 2:113–162

Punt AE, Deng RA, Dichmont CM, Kompas T and others (2010) Integrating size-structured assessment and bioeconomic management advice in Australia's northern prawn fishery. ICES J Mar Sci 67:1785–1801

Punt AE, Deng RA, Pascoe S, Dichmont CM and others (2011) Calculating optimal effort and catch trajectories for multiple species modelled using a mix of size-structured, delay-difference and biomass dynamics models. Fish Res 109:201–211

Redant F (1978) Konsumptie en produktie van post-larvale *Crangon crangon* (L.) (*Crustacea, Decapoda*) in de Belgische kustwateren. PhD dissertation, Vrije Universiteit Brussel

Rees CB (1952) Continuous plankton records: the decapod larvae in the North Sea, 1947–1949. Hull Bull Mar Ecol 3: 157–184

Reiser S, Herrmann JP, Neudecker T, Temming A (2014) Lower thermal capacity limits of the common brown shrimp (*Crangon crangon*, L.). Mar Biol 161:447–458

Rückert C (2011) Die Entwicklung, Parametrisierung und Anwendung eines Simulationsmodells für die Nordseegarnele (*Crangon crangon* L.) zur Beurteilung des Befischungszustandes. PhD dissertation, University of Hamburg

Schulte K (2015) The monitoring of the spatiotemporal distribution and movement of brown shrimp (*Crangon crangon* L.) using commercial and scientific research data. PhD dissertation, University of Hamburg

Siegel V, Damm U, Neudecker T (2008) Sex-ratio, seasonality and long-term variation in maturation and spawning of the brown shrimp *Crangon crangon* (L.) in the German Bight (North Sea). Helgol Mar Res 62:339–349

Temming A, Damm U (2002) Life cycle of *Crangon crangon* in the North Sea: a simulation of the timing of recruitment as a function of the seasonal temperature signal. Fish Oceanogr 11:45–58

Temming A, Hufnagl M (2015) Decreasing predation levels and increasing landings challenge the paradigm of non-management of North Sea brown shrimp (*Crangon crangon*). ICES J Mar Sci 72:804–823

Tetard A (1985) Elements sur la croissance de la crevette grise, *Crangon crangon* (L.), en manche-est et sud mer du nord. ICES Conference and Meeting K:17:16

Tiews K (1978) The predator–prey relationship between fish populations and the stock of brown shrimp (*Crangon crangon* L.) in the German coastal waters. Rapp P-V Reun Cons Int Explor Mer 172:250–258

Tiews K (1990) 35-Jahres-Trend (1954–1988) der Häufigkeit von 25 Fisch- und. Krebstierbeständen an der deutschen Nordseeküste. Arch FischWiss 40:39–48

Urzua A, Paschke K, Gebauer P, Anger K (2012) Seasonal and interannual variations in size, biomass and chemical composition of the eggs of North Sea shrimp, *Crangon crangon* (Decapoda: Caridea). Mar Biol 159:583–599

van der Veer HW, Bergman MJN, Dapper R, Witte JIJ (1991) Population dynamics of an intertidal 0-group flounder *Platichthys flesus* population in the western Dutch Wadden Sea. Mar Ecol Prog Ser 73:141–148

Viegas I, Martinho F, Neto J, Pardal M (2007) Population dynamics, distribution and secondary production of the brown shrimp *Crangon crangon* (L.) in a southern European estuary. Latitudinal variations. Sci Mar 71:451–460

Wear RG (1974) Incubation in British decapod Crustacea, and the effects of temperature on the rate and success of embryonic development. J Mar Biol Assoc UK 54:745–762

Welleman HC, Daan N (2001) Is the Dutch shrimp fishery sustainable? Senckenb Marit 31:321–328

Wehrtmann IS (1989) Seasonal occurrence and abundance of caridean shrimp larvae at Helgoland, German Bight. Helgol Meeresunters 43:87–112

Ye Y (1998) Assessing effects of closed seasons in tropical and subtropical penaeid shrimp fisheries using a length-based yield-per-recruit model. ICES J Mar Sci 55: 1112–1124

Editorial responsibility: Alejandro Gallego, Aberdeen, UK

Submitted: February 7, 2017; Accepted: September 5, 2017
Proofs received from author(s): November 15, 2017